



CCD UBV and Gaia DR3 based analysis of NGC 189, NGC 1758 and NGC 7762 open clusters

Talar Yontan^{a,*}, Selçuk Bilir^a, Hikmet Çakmak^a, Michel Raúl^b, Timothy Banks^{c,d}, Esin Soyduğan^{e,f},
Remziye Canbay^g, Seval Taşdemir^g

^aIstanbul University, Faculty of Science, Department of Astronomy and Space Sciences, 34116, Beyazıt, Istanbul, Turkey

^bObservatorio Astronómico Nacional, Universidad Nacional Autónoma de México, Ensenada, México

^cDepartment of Physical Science & Engineering, Harper College, 1200 W Algonquin Rd, Palatine, IL 60067, USA

^dNielsen, 200 W Jackson Blvd, Chicago, IL 60606, USA

^eÇanakkale Onsekiz Mart University, Faculty of Sciences, Department of Physics, 17100, Çanakkale, Turkey

^fÇanakkale Onsekiz Mart University, Astrophysics Research Center and Ulupınar Observatory, 17100, Çanakkale, Turkey

^gIstanbul University, Institute of Graduate Studies in Science, Programme of Astronomy and Space Sciences, 34116, Beyazıt, Istanbul, Turkey

Received 10 February 2023; Received in final form XX XXX 2023; Accepted 09 April 2023;

Available online XX XXX 2023

Abstract

This paper presents photometric, astrometric, and kinematic analyses of the open clusters NGC 189, NGC 1758 and NGC 7762 based on CCD UBV photometric and *Gaia* Data Release 3 (DR3) data. According to membership analyses, we identified 32, 57 and 106 most probable member stars with membership probabilities $P \geq 0.5$ in NGC 189, NGC 1758 and NGC 7762, respectively. The color excesses and photometric metallicities of each cluster were determined separately using UBV two-color diagrams. The color excess $E(B - V)$ is 0.590 ± 0.023 mag for NGC 189, 0.310 ± 0.022 mag for NGC 1758 and 0.640 ± 0.017 mag for NGC 7762. The photometric metallicity $[Fe/H]$ is -0.08 ± 0.03 dex for both NGC 189 and NGC 1758, and -0.12 ± 0.02 dex for NGC 7762. Distance moduli and ages of the clusters were obtained by comparing PARSEC isochrones with the color-magnitude diagrams constructed from UBV and *Gaia* photometric data. During this process, we kept as constant color excess and metallicity for each cluster. The estimated isochrone distance is 1201 ± 53 pc for NGC 189, 902 ± 33 pc for NGC 1758 and 911 ± 31 pc for NGC 7762. These are compatible with the values obtained from trigonometric parallax. Ages of the clusters are 500 ± 50 Myr, 650 ± 50 Myr and 2000 ± 200 Myr for NGC 189, NGC 1758 and NGC 7762, respectively. Galactic orbit integration of the clusters showed that NGC 1758 completely orbits outside the solar circle, while NGC 189 and NGC 7762 enter the solar circle during their orbits.

© 2023 COSPAR. Published by Elsevier Ltd All rights reserved.

Keywords: Galaxy: open clusters and associations; individual: NGC 189, NGC 1758, NGC 7762 ; Database: Gaia Photometry: color-magnitude diagram ; Galaxy kinematics; Stellar kinematics;

1. Introduction

Open clusters consist of stars initially gravitationally bound together, sharing similar positional and kinematic characteristics. Such clusters in our Galaxy are younger and of higher metallicity than the Milky Way's globular clusters. As they formed from the

*Corresponding author: Tel.: +90-212-440-0000; fax: +90-212-440-0370; Email: talar.yontan@istanbul.edu.tr, bilir@istanbul.edu.tr, hcakmak@istanbul.edu.tr, rmm@astro.unam.mx, tim.banks@nielsen.com, esoydugan@comu.edu.tr, rmzycnby@gmail.com, tasdemir.seval@ogr.iu.edu.tr

same molecular cloud, member stars share the same general distance, chemical composition and age but vary in formation masses (the initial mass function). These properties make them ‘laboratories’ allowing the study of stellar formation (Scalo, 1998; Hopkins, 2018), evolution (Donor et al., 2020), kinematics (Tarricq et al., 2021), and dynamics (Krumholz et al., 2019). Combining results from studies of many open clusters allows them to be used as tracers of the formation and chemical evolution of the Galactic disc (Adamo et al., 2020). This paper is a part of a wider programme (Bilir et al., 2006a; Bilir et al., 2010, 2016; Bostancı et al., 2015; Yontan et al., 2015, 2019, 2021; Ak et al., 2016; Banks et al., 2020; Akbulut et al., 2021; Koç et al., 2022; Yontan, 2023) applying a common methodology, building up such information. It makes use of ground-based photometry in combination with astrometric data from the *Gaia* mission (Gaia Collaboration et al., 2016, 2018, 2021, 2022), allowing the statistical removal of field stars, which act as a contaminant since they are unrelated to the cluster. The precise determination of cluster parameters requires a thorough and careful removal of this contamination, as will be outlined below.

The *Gaia* mission leads the way in the precise determination of cluster membership as well as being helpful for astrometric solutions, trigonometric parallaxes, and radial velocities of open clusters. The third data release of the European Space Agency’s *Gaia* mission (hereafter *Gaia* DR3, Gaia Collaboration et al., 2022) contains a great variety of new information, such as an extended radial velocity survey and astrophysical characterisation of *Gaia* objects. Due to the longer period data have been collected over, *Gaia* DR3 is of higher quality than the earlier *Gaia* DR2 (Gaia Collaboration et al., 2018) and *Gaia* DR1 (Gaia Collaboration et al., 2016) releases. As the first part of *Gaia* DR3, the third (early) data release *Gaia* EDR3 (Gaia Collaboration et al., 2021) contains astrometric, photometric and spectroscopic data for around 1.8 billion objects. *Gaia* DR3 has the same source catalogue as *Gaia* EDR3 but supplements it in the sense of the large variety of new data products. For many celestial objects, *Gaia* DR3 includes their astrophysical parameters estimated from parallaxes, broadband photometry, and mean radial velocity spectra (Gaia Collaboration et al., 2022). In *Gaia* DR3, trigonometric parallax errors are 0.02-0.07 mas for $G \leq 17$ mag, 0.5 mas for $G = 20$ mag and reach 1.3 mas for $G = 21$ mag. The proper-motion errors are $0.02 - 0.07 \text{ mas yr}^{-1}$, reaching up to 0.5 mas yr^{-1} for $G = 20$ mag and 1.4 mas yr^{-1} for $G = 21$ mag.

This study explores the clusters NGC 189, NGC 1758 and NGC 7762. These clusters were selected from an ongoing *UBVRI* photometric survey of Galactic stellar clusters at the San Pedro Martir Observatory. The current study constitutes the second of our paper series based on this survey (Yontan, 2023), as part of the wider programme described above. The paper outlines an analysis combining CCD *UBV* and recent *Gaia* DR3 photometric and astrometric data. Independent methods, such as those estimating the color excess and metallicity parameters, reduced possible parameter degeneracy and lead to reliable estimates for astrophysical parameters of all three clusters.

1.1. NGC 189

NGC 189 ($\alpha = 00^{\text{h}}39^{\text{m}}32^{\text{s}}$, $\delta = +61^{\circ}05'24''$, $l = 121^{\circ}4938$, $b = -01^{\circ}7485$, SIMBAD¹ J2000) was likely discovered by Caroline Herschel in 1783 (Hoskin, 2006). The cluster was examined by Alter (1944) who mentioned that the cluster lies in a comparatively rich region, and estimated its distance as 1490 ± 200 pc and diameter ~ 1.6 pc. Balazs (1961) presented color-magnitude and two-color diagrams for the cluster, estimating a distance of 790 pc. de la Fuente Marcos & de la Fuente Marcos (2009) noted NGC 189 in their list of candidate binary clusters, matching it with ASCC 4 (Kharchenko et al., 2005). The cluster has been included in many subsequent studies, such as those based on *Gaia* data (Cantat-Gaudin et al., 2018; Liu & Pang, 2019; Cantat-Gaudin et al., 2020;

¹<https://simbad.unistra.fr/simbad/>

Dias et al., 2021; Poggio et al., 2021), with results listed in Table 1 for ease of comparison. The table also provides comparisons for NGC 1758 and NGC 7762.

1.2. NGC 1758

Dreyer (1888) noted three overlapping open clusters: NGC 1746, NGC 1750 and NGC 1758 ($\alpha = 05^{\text{h}}04^{\text{m}}42^{\text{s}}$, $\delta = +23^{\circ}48'47''$, $l = 179^{\circ}1584$, $b = -10^{\circ}4597$, SIMBAD J2000). Since then there has been disagreement between authors of the existence of one or more of these clusters. Cuffey & Shapley (1937) presented blue and red photographic photometry for NGC 1746 (down to $R \sim 14^{\text{th}}$ mag), with no mention of either NGC 1750 or NGC 1758, commenting that NGC 1746 is a thin and asymmetrical cluster. Straizys et al. (1992) conducted Vilnius photometry (Straizys, 1992) down to $V \sim 13$ of 116 stars in the vicinity of the three clusters. They concluded that NGC 1746 is probably not a cluster and were not confident that the other two groupings were real as well. Tian et al. (1998) concluded there were only two clusters (NGC 1750 and NGC 1758). Galadi-Enriquez et al. (1998a,b) disagreed with Cuffey & Shapley's identification of NGC 1746 based on their Johnson-Cousins CCD *UBVRI* photometry, which they judged as completed down to $V \sim 18.5$ mag. Galadi-Enriquez et al. (1998b) wrote that there was no photometric evidence for the cluster NGC 1746 and that Cuffey & Shapley (1937) had erroneously assigned a stellar concentration of NGC 1758 as the asymmetric nucleus of NGC 1746. Galadí-Enríquez et al. (1999) noted NGC 1750 and NGC 1758 to be poor and loose, concluding from their relative velocity, separation, and age difference that they are physically independent clusters. Landolt & Africano (2010) undertook *UBV* broadband photometry for 19 stars in the direction of the suspected clusters, admitting confusion on the number of clusters that might be present. Table 1 succinctly presents parameters from the literature for NGC 1758, such as color excess, distance moduli, distances, iron abundances, age, proper-motion components, and radial velocity.

1.3. NGC 7762

Chincarini (1966) presented *UBV* photographic photometry of NGC 7762 ($\alpha = 23^{\text{h}}49^{\text{m}}53^{\text{s}}$, $\delta = +68^{\circ}02'06''$, $l = 117^{\circ}2060$, $b = 05^{\circ}8501$, SIMBAD J2000), classifying the cluster as Trumpler class II 1 m U, 1020 pc away and of diameter 3.5 pc. Patat & Carraro (1995) reported CCD *BV* photometry of the central region of the cluster, commenting that it was very loose in structure and large. They concluded that NGC 7762 is of intermediate age, being ~ 1.8 Gyr old and ~ 800 pc distance. Szabo (1999) identified photometrically variable stars in the cluster. No δ Scuti variables were found, which they concluded as confirming that NGC 7762 is older than 800 Myr in age. Bonatto & Bica (2011) presented a proper motion distribution function for the cluster, characterised as a single Gaussian. Casamiquela et al. (2016) undertook high-resolution spectroscopy of the cluster, providing estimates for U_s , V_s and W_s cluster velocities in the Cartesian Galactocentric frame, while Reddy & Lambert (2019) analysed high-dispersion Echelle spectra ($R=60\,000$) of red giant members to derive a $[\text{Fe}/\text{H}]$ value of -0.07 ± 0.03 dex for NGC 7762.

2. Observations

2.1. CCD *UBV* photometric data

The observations of these three clusters were collected by R. Michel at the San Pedro Martir Observatory as part of an ongoing² *UBVRI* photometric survey of Galactic stellar clusters. In the case of these clusters, the 0.84-m ($f/15$) Ritchey–Chrétien telescope was employed along with the Mexman filter wheel and the Marconi 5 camera (a 2048×2048 $15\mu\text{m}$ square-pixel E2V CCD31-42 detector with a gain of $2.38e^-/\text{ADU}$ and a readout noise of $4.02e^-$ with 2×2 binning employed, providing an unvignetted field of

²http://bufadora.astrofen.unam.mx/~rmm/SPMO_UBVRI_Survey/Clusters_All.html

Table 1. Fundamental parameters for NGC 189, NGC 1758, and NGC 7762 derived in this study and compiled from the literature: Color excesses ($E(B - V)$), distance moduli (μ), distances (d), iron abundances ([Fe/H]), age (t), proper-motion components ($\langle\mu_\alpha \cos \delta\rangle$, $\langle\mu_\delta\rangle$), radial velocity (V_γ) and reference (Ref).

NGC 189								
$E(B - V)$ (mag)	μ (mag)	d (pc)	[Fe/H] (dex)	t (Myr)	$\langle\mu_\alpha \cos \delta\rangle$ (mas yr ⁻¹)	$\langle\mu_\delta\rangle$ (mas yr ⁻¹)	V_γ (km s ⁻¹)	Ref
0.44	11.52	1080	—	2	—	—	—	(01)
0.56	11.35	860	—	—	—	—	—	(02)
0.700	—	1300	—	510	-0.31	-2.71	—	(03)
—	—	—	—	—	-0.36±0.59	-3.02±0.10	—	(04)
0.700	—	1300	—	510±60	—	—	—	(05)
0.420	—	752	—	10	+0.34±3.23	-1.11±1.93	—	(06)
0.323	—	1088	—	380	+2.761±1.368	-2.398±0.947	—	(07)
—	—	1248 ⁺¹⁷⁹ ₋₁₃₈	—	—	+0.338±0.016	-3.306±0.023	—	(08)
—	—	1248 ⁺¹⁷⁹ ₋₁₃₈	—	—	+0.338±0.016	-3.306±0.023	-28.47±0.75	(09)
—	—	1302±46	—	562±34	+0.323±0.280	-3.307±0.195	—	(10)
0.497	11.991	1228	—	400	+0.338±0.071	-3.306±0.109	—	(11)
—	—	1248 ⁺¹⁷⁹ ₋₁₃₈	—	—	+0.338±0.016	-3.306±0.023	—	(12)
0.602±0.045	—	1247±49	0.119±0.152	490±490	+0.336±0.120	-3.315±0.176	-29.391±0.534	(13)
0.590±0.023	12.227±0.094	1201±53	-0.08±0.03	500±50	+0.352±0.032	-3.412±0.038	-29.60±0.32	(14)
NGC 1758								
0.37±0.02	—	680±24	—	—	—	—	—	(15)
0.34±0.07	10.45	760	—	400±100	+0.70	-8.1	—	(16)
0.34	—	760	—	—	—	—	—	(17)
—	—	—	—	—	-0.61±2.32	-3.57±0.76	—	(04)
0.34	—	760	—	400	-0.72±4.83	-2.61±3.31	—	(06)
0.327	—	621	—	540	-0.068±0.012	+1.335±0.116	—	(07)
—	—	884 ⁺⁸⁵ ₋₇₂	—	—	+3.156±0.013	-3.465±0.010	—	(08)
—	—	907±56	—	355±21	+3.148±0.257	-3.474±0.204	—	(10)
0.299±0.007	10.771±0.025	931±11	0.00	550 ⁺²⁴ ₋₃₉	—	—	—	(18)
0.300	10.67	885	—	355	+3.156±0.146	-3.465±0.129	—	(11)
—	—	884 ⁺⁸⁵ ₋₇₂	—	—	+3.156±0.013	-3.465±0.010	—	(12)
0.388±0.019	—	864±29	0.098±0.073	540±70	+3.156±0.157	-3.470±0.118	17.840±9.887	(13)
0.310±0.022	10.736±0.078	902±33	-0.08±0.03	650±50	+3.141±0.035	-3.507±0.025	6.80±2.90	(14)
NGC 7762								
1.02	13.10	1020	—	155	—	—	—	(19)
0.90	12.20	800	—	1800	—	—	—	(20)
0.66 ^{+0.08} _{-0.09}	11.52 ^{+0.42} _{-0.75}	780 ⁺²⁰⁰ ₋₃₀₀	—	2000	—	—	—	(21)
0.59	11.3 ^{+0.5} _{-0.8}	800 ⁺²⁰⁰ ₋₃₀₀	0.00	2500 ⁺²⁰⁰⁰ ₋₇₀₀	—	—	—	(22)
0.550	—	780	—	2360±180	-2.88	0.00	—	(03)
—	—	—	—	—	—	—	-45.7±0.7	(23)
0.550	—	780	—	2100±100	—	—	—	(05)
—	—	780	0.01±0.04	2500	—	—	—	(24)
—	—	970 ⁺¹⁰⁴ ₋₈₆	—	—	+1.452±0.010	-4.016±0.010	—	(08)
—	—	970 ⁺¹⁰⁴ ₋₈₆	—	—	+1.452±0.010	-4.016±0.010	-45.40±0.14	(09)
—	—	—	-0.07±0.04	—	—	—	—	(25)
—	—	1005±41	—	2630±158	+1.478±0.274	+4.002±0.248	—	(10)
0.616	11.76	897	—	2050	+1.452±0.010	-4.016±0.010	—	(11)
—	—	970 ⁺¹⁰⁴ ₋₈₆	—	—	+1.452±0.010	-4.016±0.010	—	(12)
0.840±0.017	—	957±13	-0.056±0.103	1100±370	+1.461±0.203	+4.006±0.198	-45.438±0.492	(13)
0.640±0.017	11.781±0.072	911±31	-0.12±0.02	2000±200	+1.489±0.023	+3.962±0.024	-46.61±0.10	(14)

(01) Lindoff (1968), (02) Becker & Fenkart (1971), (03) Kharchenko et al. (2013), (04) Dias et al. (2014), (05) Joshi et al. (2016), (06) Sampedro et al. (2017), (07) Loktin & Popova (2017), (08) Cantat-Gaudin et al. (2018), (09) Soubiran et al. (2018), (10) Liu & Pang (2019), (11) Cantat-Gaudin et al. (2020), (12) Cantat-Gaudin & Anders (2020), (13) Dias et al. (2021), (14) This study, (15) Straižys et al. (1992), (16) Galadi-Enriquez et al. (1998a), (17) Straižys et al. (2003), (18) Bossini et al. (2019), (19) Chincarini (1966), (20) Patat & Carraro (1995), (21) Maciejewski & Niedzielski (2007), (22) Maciejewski et al. (2008), (23) Casamiquela et al. (2016), (24) Casamiquela et al. (2017), (25) Reddy & Lambert (2019)

view of 9.3×9.3 arcmin²). Exposure times were 2, 20 and 200s for both filters *I* and *R*; 3, 30 and 300 for filter *V*; 5, 50 and 500s for filter *B*; and 10, 100 and 1000s for filter *U*.

The observations were carried out during photometric conditions across different observing runs. NGC 189 was observed on 22 September 2015. NGC 1758 was observed on 4 February 2016, and NGC 7762 on 17 January 2015. Landolt's standard stars (Landolt, 2009) were also observed, both at the meridian and at around two airmasses, in order to properly determine the transformation equations. Flat fields were taken at the beginning and the end of each night. Bias images were obtained between cluster observations. Data reduction with point spread function (PSF) photometry was carried out with the IRAF/DAOPHOT packages. The transformation equations recommended by Stetson et al. (2019) were employed.

2.2. Gaia Data

The *Gaia* DR3 database (Gaia Collaboration et al., 2022) was used together with CCD *UBV* photometry to accomplish astrometric, photometric, and kinematic analyses of NGC 189, NGC 1758 and NGC 7762. We extracted data from the *Gaia* DR3 database within a 40 arcmin radius (centred on literature cluster centres) and matched it with the *UBV* data according to stars' equatorial coordinates, taking into account distances between coordinates of less than 5 arcsec between the data sets. Hence we created photometric and astrometric catalogues for the three clusters containing the detected stars' positions (α, δ), apparent *V* magnitudes, *U* – *B* and *B* – *V* color indices, *Gaia* DR3 proper-motion components ($\mu_\alpha \cos \delta, \mu_\delta$), trigonometric parallaxes (ϖ), apparent *G* magnitudes, and $G_{BP} - G_{RP}$ color indices as well as the membership probabilities (*P*) which were calculated in this study (Table 2, page 8). *UBV* and *Gaia* based photometric and astrometric data for each star located in the cluster areas are available electronically for NGC 189, NGC 1758 and NGC 7762.³ $9'.3 \times 9'.3$ field of view optical images for the clusters under study are presented in Figure 1. The photometric errors in *UBV* and *Gaia* DR3 data were adopted as internal errors, which are the uncertainties of the instrumental magnitudes of the stars. The mean errors in the *UBV* and *Gaia* DR3 photometric data were calculated as functions of *V* apparent magnitude. The results are given in Table 3 (on page 9). We found that the mean errors in *V* magnitude reach up to 0.1 mag, while for the *U* – *B* and *B* – *V* color indices, the mean errors are about 0.3 mag and 0.2 mag, respectively, for the three clusters. The mean errors in *G* magnitudes reach up to 0.01 mag, whereas in the $G_{BP} - G_{RP}$ color index they are less than 0.25 mag for the stars $V \leq 22$ mag (see Table 3).

Crowding by other stellar images in CCD frames can prevent the detection of faint stars in the clusters. This crowding will lower the number of detected faint stars, dropping the 'completeness' from unity (where all stars are detected). Understanding the decreasing completeness of the measured stellar counts with increasing magnitude is necessary to derive reliable astrophysical parameters of open clusters. To define photometric completeness limits for the three clusters, we constructed histograms of the observed *G* and *V* magnitudes (Fig. 2). We compared the observed *G* magnitude histograms with the *Gaia* DR3 data for the $9'.3 \times 9'.3$ region on the sky matching the fields observed from the ground. All histograms for stellar counts are shown in Fig. 2: the black solid lines show the observational stellar distributions by magnitude bin in *V* and *G*, while the red solid lines (see in Fig. 2b, 2d and 2f) represent the *Gaia* DR3 based stellar counts. It can be seen in Fig. 2b, 2d and 2f that the numbers of stars detected in the three cluster regions are well matched with the *Gaia* DR3 stellar distributions up to fainter magnitudes. The magnitudes adopted as photometric completeness limits are $V = 19$ mag for NGC 189 and NGC 7762, $V = 18$ mag for NGC 1758 and $G = 18$ mag for all clusters (the limits are the vertical dashed lines in all panels of Fig. 2). In Fig. 2b, 2d and 2f the number of stars decreases with the increasing crowding of low-mass stars beyond the adopted completeness limits. Observational techniques, telescope-detector

³The complete tables can be obtained from VizieR electronically.

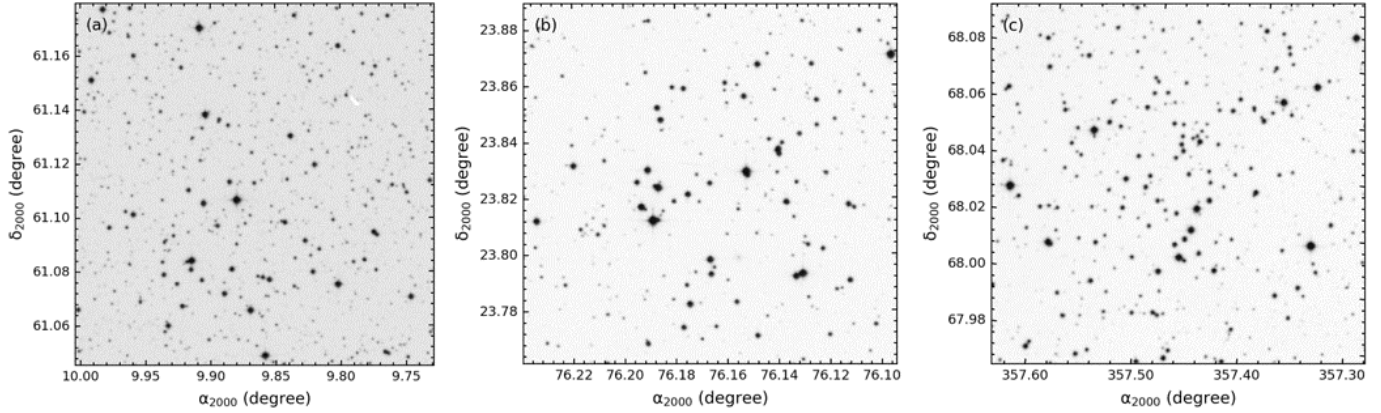


Fig. 1. Identification charts of NGC 189 (a), NGC 1758 (b) and NGC 7762 (c). The field of view of the charts are $9'.3 \times 9'.3$. North is up and East left.

combinations, and telescope qualities used in ground and space-based observations have an impact on detecting stars, especially at fainter magnitudes. This could clarify the reason why the stellar counts fainter than $G > 18$ mag in the *Gaia* space-based observations are greater than the number of detected stars in the study.

2.3. Spatial Structures of the Clusters

Before investigating the spatial structure of the three clusters, we determined the central equatorial coordinates (α , δ) by applying the star count method. The calculated central coordinates for NGC 189 and NGC 7762 are in agreement with the values given by Cantat-Gaudin et al. (2020). Results are listed in Table 4 (on page 9) for the three clusters.

To measure the extent of the clusters, we used *Gaia* DR3 data within 40 arcmin of the derived cluster centres. Estimation of the structural parameters of NGC 189, NGC 1758 and NGC 7762 employed a radial density profile (RDP) for each cluster as shown in Figure 3 (page 10). We divided a cluster's area into several concentric rings around the cluster center that we estimated in the study and calculated the stellar number density ($\rho(r)$) for an i th ring as $R_i = N_i/A_i$, where N_i and A_i indicate the number of stars in that circle and the surface area, respectively. Uncertainties in the stellar number densities were estimated by Poisson statistics ($1/\sqrt{N}$, where N is the number of stars). We fitted the empirical RDP of King (1962), which is expressed by the following formula:

$$\rho(r) = f_{bg} + \frac{f_0}{1 + (r/r_c)^2} \quad (1)$$

where f_{bg} is the background stellar density, f_0 the central stellar density and r_c the core radius of the cluster. The RDP fitting procedure utilized a χ^2 minimization method. The derived structural parameters for each cluster are listed in Table 4 (page 9). The best-fit RDP of each cluster is represented by a solid line in the corresponding sub-figures of Figure 3. We estimated the limiting radii (r_{lim}^{obs}) according to a visual review of RDP. We identified that the limiting radius as the point where the background stellar density (shown by the horizontal grey band in Figure 3) matches with or equals the RDP. We therefore considered the limiting radii as $r_{lim}^{obs} = 4'$ for NGC 189, $r_{lim}^{obs} = 7'$ for NGC 1758 and $r_{lim}^{obs} = 15'$ for NGC 7762. To determine the mathematical accuracy of these visually determined r_{lim}^{obs} values, we used the equation of Bukowiecki et al. (2011):

$$r_{lim} = r_c \sqrt{\frac{f_0}{3\sigma_{bg}} - 1} \quad (2)$$

We therefore calculated the limiting radii (r_{lim}^{cal}) as $3'.55$ for NGC 189, $7'.18$ for NGC 1758 and $14'.95$ for NGC 7762 (see also Table 4). The fact that the calculated limiting radii are compatible with the observational values, and that the correlation coefficients

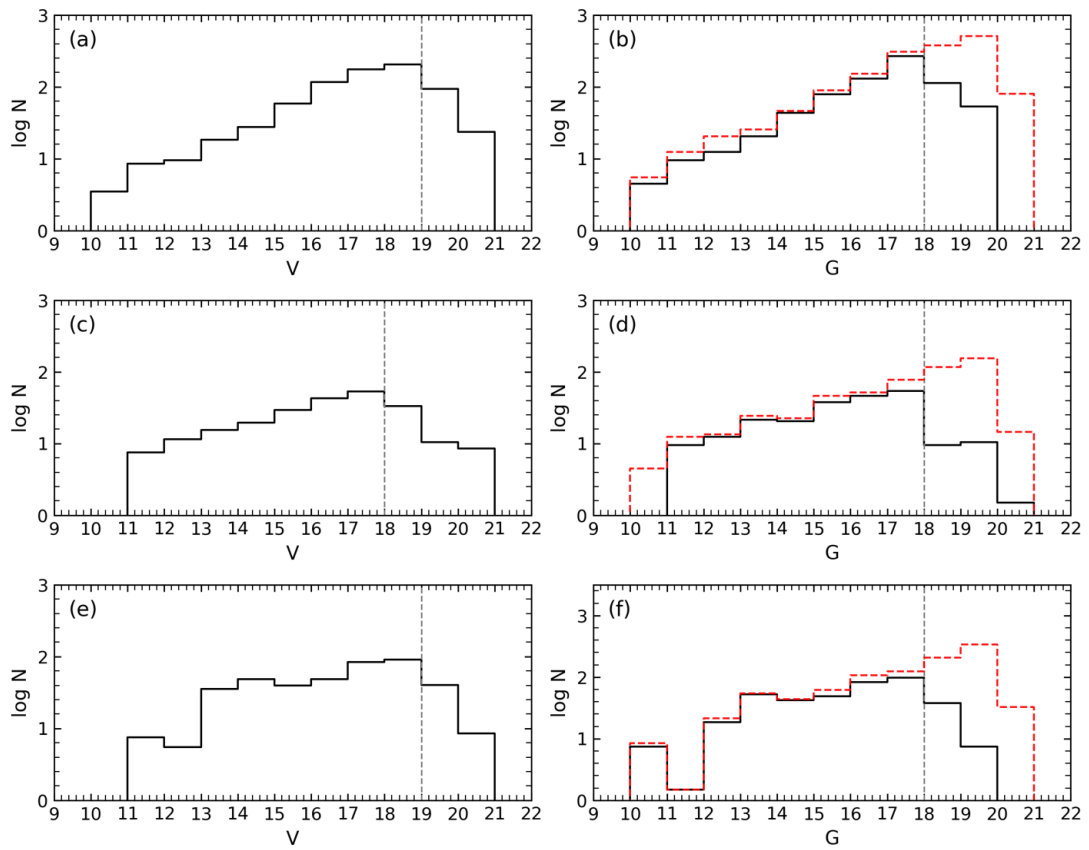


Fig. 2. Histograms of NGC 189 (a, b), NGC 1758 (c, d) and NGC 7762 (e, f) per magnitude bin in the filters V (black lines) and G (red lines). The vertical dashed lines indicate the adopted faint limiting apparent magnitudes in the V and G bands.

Table 2. The photometric and astrometric catalogues for NGC 189, NGC 1758, and NGC 7762 members

NGC 189											
ID	RA	DEC	V	$U - B$	$B - V$	G	$G_{BP} - G_{RP}$	$\mu_{\alpha} \cos \delta$	μ_{δ}	ϖ	P
	(hh:mm:ss.ss)	(dd:mm:ss.ss)	(mag)	(mag)	(mag)	(mag)	(mag)	(mas yr ⁻¹)	(mas yr ⁻¹)	(mas)	
001	00:39:31.15	+61:06:23.67	10.933(0.008)	0.522(0.065)	0.863(0.064)	10.844(0.011)	1.302(0.005)	—	—	—	—
002	00:39:37.97	+61:10:12.88	11.221(0.025)	0.202(0.045)	0.590(0.050)	11.210(0.009)	0.854(0.005)	—	—	—	—
003	00:39:28.64	+61:03:56.79	11.831(0.029)	0.331(0.040)	0.443(0.047)	11.789(0.003)	0.611(0.005)	-6.112(0.012)	0.382(0.014)	1.097(0.013)	0.00
004	00:39:12.49	+61:04:31.15	11.837(0.019)	0.428(0.038)	0.628(0.041)	11.655(0.003)	0.935(0.005)	-0.628(0.037)	-3.088(0.043)	0.859(0.39)	0.00
...
...
733	00:39:45.99	+61:06:59.69	21.435(0.179)	—	0.945(0.234)	20.808(0.012)	1.424(0.210)	-2.461(01.585)	1.607(1.503)	0.727(1.303)	0.00
734	00:39:13.34	+61:07:07.29	21.583(0.165)	—	0.673(0.211)	—	—	—	—	—	—
735	00:39:04.22	+61:05:07.37	21.587(0.187)	—	1.428(0.333)	20.924(0.022)	1.843(0.368)	—	—	—	—
736	00:39:25.31	+61:05:25.71	21.655(0.272)	—	0.886(0.317)	20.744(0.010)	1.340(0.176)	-2.047(1.038)	1.115(1.132)	0.025(0.925)	0.01
NGC 1758											
001	05:04:22.95	+23:52:14.48	11.105(0.074)	0.267(0.101)	0.429(0.111)	11.009(0.003)	0.641(0.005)	3.112(0.022)	-3.649(0.016)	1.179(0.020)	0.99
002	05:04:31.31	+23:47:34.80	11.346(0.071)	0.254(0.092)	0.413(0.103)	11.266(0.003)	0.620(0.005)	3.019(0.025)	-3.438(0.019)	1.117(0.021)	1.00
003	05:04:46.38	+23:49:00.94	12.101(0.048)	0.334(0.068)	0.434(0.075)	11.997(0.003)	0.662(0.005)	3.136(0.018)	-3.547(0.013)	1.138(0.016)	1.00
004	05:04:56.17	+23:48:43.25	12.334(0.045)	0.322(0.062)	0.401(0.070)	12.200(0.003)	0.633(0.005)	2.927(0.020)	-3.330(0.014)	1.159(0.017)	0.99
...
...
226	05:04:26.84	+23:46:42.32	21.308(0.127)	—	0.882(0.193)	21.004(0.025)	0.854(0.444)	—	—	—	0.47
227	05:04:40.16	+23:51:46.41	21.359(0.132)	—	0.253(0.176)	—	—	—	—	—	—
228	05:04:37.57	+23:48:04.10	21.385(0.162)	—	0.720(0.217)	20.724(0.012)	0.641(0.260)	0.349 (2.355)	-0.566(1.632)	-1.666(1.586)	0.00
229	05:04:46.99	+23:47:08.86	21.585(0.170)	—	0.939(0.260)	20.696(0.011)	0.968(0.427)	-0.428(1.428)	-1.276(1.079)	0.279 (1.264)	0.00
NGC 7762											
001	23:49:21.67	+68:01:01.74	11.705(0.011)	1.218(0.012)	1.700(0.013)	10.794(0.003)	2.131(0.005)	1.290(0.018)	3.747 (0.019)	1.034(0.017)	0.98
002	23:50:31.42	+68:01:41.56	11.725(0.017)	1.204(0.014)	1.609(0.019)	10.904(0.003)	2.010(0.005)	1.345(0.021)	4.134 (0.022)	1.017(0.019)	0.98
003	23:50:13.51	+68:03:02.70	12.199(0.012)	1.094(0.009)	1.559(0.013)	11.482(0.003)	1.925(0.005)	3.135(0.015)	-3.269(0.016)	1.034(0.014)	0.00
004	23:49:23.53	+68:04:24.88	12.471(0.052)	0.726(0.023)	1.266(0.056)	11.835(0.003)	1.763(0.005)	3.358(0.177)	0.207 (0.182)	1.661(0.174)	0.00
...
...
403	23:50:01.51	+68:01:21.45	21.300(0.146)	—	0.457(0.190)	—	—	—	—	—	—
404	23:49:28.77	+68:01:48.92	21.390(0.178)	—	1.349(0.296)	20.462(0.007)	2.040(0.138)	-0.890(0.759)	-1.817(0.634)	-0.506(0.581)	0.00
405	23:50:11.55	+68:01:49.47	21.491(0.205)	—	1.227(0.326)	—	—	—	—	—	—
406	23:49:34.88	+67:58:37.81	21.912(0.267)	—	0.575(0.355)	20.838(0.011)	1.772(0.235)	-1.741(1.444)	1.070 (1.400)	-1.654(1.290)	0.00

of the King models with the best-fit model parameters to the data are higher than $R^2 = 0.95$, indicates that the estimated structural parameters are well estimated.

2.4. Color-Magnitude diagrams and membership probabilities of stars

Open clusters are located through the Galactic plane, leading to them usually being affected by field star contamination. To obtain fundamental cluster parameters more precisely, it is important to separate cluster members from foreground/background non-member stars. Stars in an open cluster are formed under the same physical conditions, and they move in the same general vectorial directions in space. These properties make proper-motion components useful tools to separate cluster members (Bisht et al., 2020) from field stars. Thanks to *Gaia* DR3's high accuracy astrometric data, membership analyses give reliable results if carefully made. To determine membership probabilities (P) of stars located in the direction of the three clusters, we performed the Unsupervised Photometric Membership Assignment in Stellar Clusters (UPMASK; Krone-Martins & Moitinho, 2014) method on *Gaia* DR3 astrometric data. The method was used in previous studies by various researchers (Cantat-Gaudin et al., 2018, 2020; Castro-Ginard et al., 2018, 2019, 2020; Banks et al., 2020; Akbulut et al., 2021; Wang et al., 2022; Yontan, 2023). UPMASK is a k -means clustering method which considers the proper-motion components as well as the trigonometric parallaxes of the stars. This technique allows the detection of similar groups of stars, together with estimates of membership probabilities for these groups. To determine the most probable members for NGC 189, NGC 1758 and NGC 7762 and to evaluate membership probabilities, we ran 100 iterations of UPMASK which considered each detected star's astrometric measurements (α , δ , $\mu_{\alpha} \cos \delta$, μ_{δ} , ϖ) and their uncertainties. We determined 79 likely member stars for NGC 189, 61 for NGC 1758 and 118 stars for NGC 7762 as the most probable cluster members with membership probabilities $P \geq 0.5$ and brighter than the photometric completeness limits described

Table 3. Mean internal photometric errors per magnitude bin in V brightness for the three open clusters.

NGC 189						
V	N	σ_V	σ_{U-B}	σ_{B-V}	σ_G	$\sigma_{G_{BP}-G_{RP}}$
(10, 12]	4	0.020	0.047	0.050	0.006	0.005
(12, 14]	17	0.015	0.026	0.028	0.003	0.005
(14, 15]	18	0.009	0.015	0.014	0.003	0.005
(15, 16]	27	0.009	0.018	0.012	0.003	0.007
(16, 17]	58	0.011	0.024	0.014	0.003	0.006
(17, 18]	117	0.015	0.041	0.021	0.003	0.010
(18, 19]	175	0.025	0.089	0.037	0.003	0.021
(19, 20]	204	0.038	0.171	0.062	0.003	0.039
(20, 22]	116	0.103	0.295	0.160	0.005	0.100
NGC 1758						
V	N	σ_V	σ_{U-B}	σ_{B-V}	σ_G	$\sigma_{G_{BP}-G_{RP}}$
(10, 12]	4	0.072	0.097	0.107	0.003	0.005
(12, 14]	18	0.020	0.042	0.044	0.003	0.005
(14, 15]	15	0.010	0.022	0.021	0.003	0.005
(15, 16]	19	0.006	0.013	0.009	0.003	0.006
(16, 17]	29	0.011	0.017	0.014	0.003	0.008
(17, 18]	42	0.012	0.040	0.020	0.003	0.014
(18, 19]	53	0.021	0.074	0.032	0.003	0.030
(19, 20]	32	0.036	0.082	0.073	0.004	0.065
(20, 22]	17	0.099	0.226	0.158	0.010	0.240
NGC 7762						
V	N	σ_V	σ_{U-B}	σ_{B-V}	σ_G	$\sigma_{G_{BP}-G_{RP}}$
(10, 12]	2	0.014	0.013	0.016	0.003	0.005
(12, 14]	12	0.019	0.013	0.021	0.003	0.005
(14, 15]	35	0.014	0.013	0.016	0.003	0.005
(15, 16]	48	0.008	0.016	0.010	0.003	0.006
(16, 17]	39	0.010	0.031	0.014	0.003	0.006
(17, 18]	48	0.014	0.077	0.026	0.003	0.011
(18, 19]	84	0.022	0.133	0.043	0.003	0.022
(19, 20]	90	0.038	0.186	0.076	0.003	0.048
(20, 22]	48	0.099	—	0.184	0.005	0.100

Table 4. The structural parameters of the three open clusters according to King (1962) model analyses: (α, δ) , f_0 , f_{bg} , r_c , r_{lim}^{obs} , r_{lim}^{cal} and R^2 are equatorial coordinates, central stellar densities, the background stellar densities, the core radius, observational limiting radius, calculated limiting radius and correlation coefficients, respectively.

Cluster	α_{J2000} (hh:mm:ss.ss)	δ_{J2000} (dd:mm:ss.ss)	f_0 (stars arcmin ⁻²)	f_{bg} (stars arcmin ⁻²)	r_c (arcmin)	r_{lim}^{obs} (arcmin)	r_{lim}^{cal} (arcmin)	R^2
NGC 189	00:39:27.89	+61:06:46.35	4.86±0.41	12.38±0.08	0.81±0.12	4	3.55	0.959
NGC 1758	05:04:42.00	+23:48:46.90	2.97±0.17	3.14±0.08	2.13±0.28	7	7.18	0.951
NGC 7762	23:49:53.00	+68:02:06.00	4.91±0.24	4.92±0.13	4.39±0.46	15	14.95	0.957

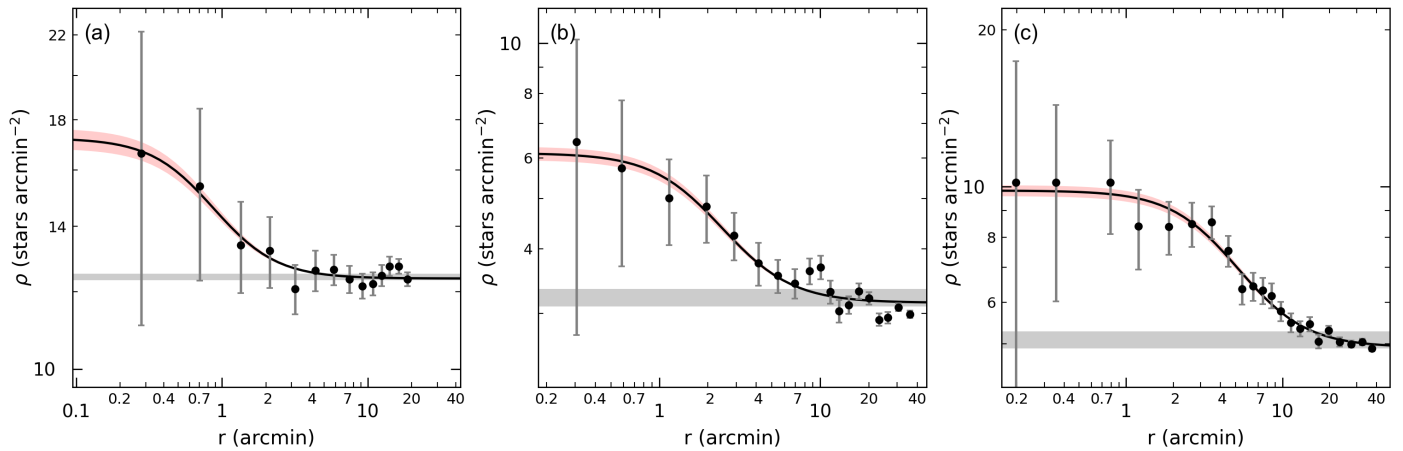


Fig. 3. The stellar density distribution of the clusters NGC 189 (a), NGC 1758 (b), and NGC 7762 (c). The fitted black curve shows the RDP profile of King (1962), whereas the horizontal grey band represents the background stellar density. The 1σ King fit uncertainty is pictured by the red-shaded area.

above.

The observed color-magnitude diagrams (CMDs) are useful tools to derive age, distance, and other key parameters for open star clusters. In other respects, CMDs created in different photometric systems are effective tools to explore the main sequence, turn-off, and giant region of star clusters. In this study, we used UBV based CMDs to take into account the possible ‘contamination’ by binary stars in the main sequence of the three clusters. Considering the stars with the probabilities $P \geq 0.5$, we constructed $V \times (B - V)$ CMDs and fitted the Zero Age Main-Sequence (ZAMS) line of Sung et al. (2013) to these diagrams through visual inspection according to most probable main-sequence stars. We shifted the ZAMS by 0.75 mag over the brighter stars to adjust for possible binary star contamination by making sure that we chose clearly the most probable main sequence, turn-off and giant members. Consequently, with constraints on the completeness-estimated V magnitude limits and fitted ZAMS, we obtained 32 member stars for NGC 189, 57 for NGC 1758 and 106 for NGC 7762 with membership probabilities $P \geq 0.5$. The $V \times (B - V)$ diagrams with fitted ZAMS and distribution of both field and cluster stars are shown in Figs. 4a (for NGC 189), 4c (for NGC 1758) and 4e (for NGC 7762). The stellar distributions using the *Gaia* based photometry are shown in Figs. 4b (for NGC 189), 4d (for NGC 1758) and 4f (for NGC 7762).

Figure 5 plots the membership probabilities of detected stars as a function of stellar numbers. To determine the locations of the most probable cluster members and the field stars in proper-motion space, we drew vector point diagrams (VPDs) for the three clusters (see Fig. 6). It can be seen from the figure that all three clusters are clearly separated from their field stars. In Fig. 6, the intersection of the blue dashed lines indicates the mean proper-motion values estimated from the stars with membership probabilities $P \geq 0.5$. The mean proper-motion components are listed in Table 5. These results are in good agreement with the values of previous studies based on *Gaia* observations for the three clusters (see Table 1). To estimate the astrometric distance of each cluster, we used trigonometric parallaxes considering the cluster members (i.e., stars with $P \geq 0.5$). We constructed the trigonometric parallax histograms using these members and calculated the mean values for each cluster by fitting Gaussian functions to the distributions as shown in Fig. 7. As a result, the mean trigonometric parallax values were obtained as $\varpi = 0.778 \pm 0.051$ mas for NGC 189, $\varpi = 1.150 \pm 0.076$ mas for NGC 1758 and $\varpi = 1.033 \pm 0.025$ mas for NGC 7762. By applying the linear equation of $d(\text{pc}) = 1000/\varpi$ (mas) to the mean trigonometric parallaxes, we derived the astrometric distances as $d_{\varpi} = 1285 \pm 84$ pc for NGC 189, $d_{\varpi} = 870 \pm 57$ pc for NGC 1758 and $d_{\varpi} = 968 \pm 23$ pc for NGC 7762. We obtained similar mean parallax values for NGC 189 and NGC 7762 compared to Cantat-Gaudin et al. (2020) and Cantat-Gaudin & Anders (2020). NGC 1758 was not examined

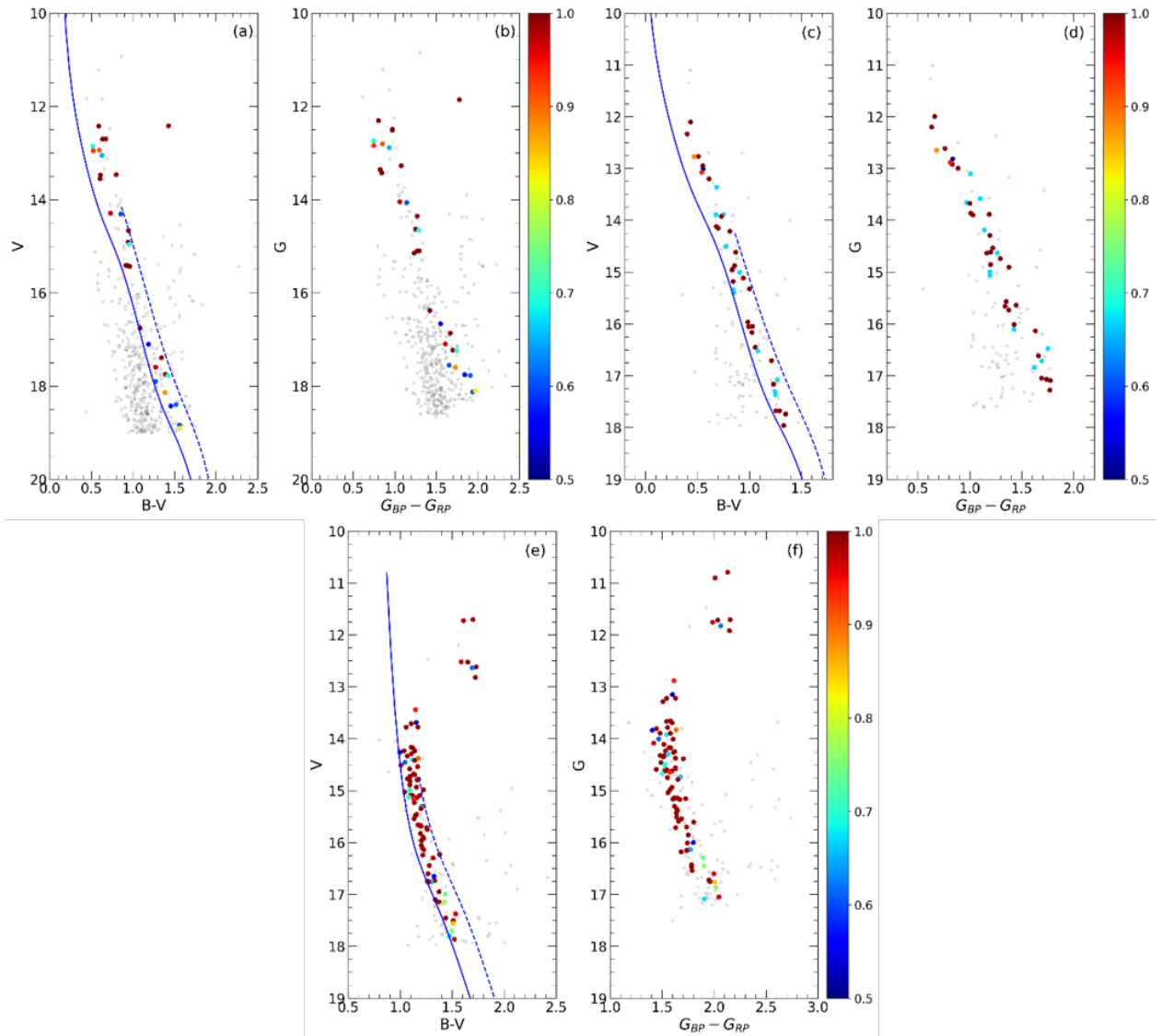


Fig. 4. CMDs of NGC 189 (a, b), NGC 1758 (c, d), and NGC 7762 (e, f) based on *UBV* (a, c, e) and *Gaia* DR3 photometry (b, d, f). The blue dashed lines show the ZAMS (Sung et al., 2013) including the binary star contamination. The membership probabilities of stars are represented with different colors, the member stars are located within $r_{\text{lim}} = 4'$, $r_{\text{lim}} = 7'$, and $r_{\text{lim}} = 15'$ of the cluster centres calculated for NGC 189, NGC 1758 and NGC 7762, respectively. The stars with low membership probabilities ($P < 0.5$) were indicated with grey dots.

by those studies.

3. Astrophysical Parameters

In this section, we sum up the methods followed to determine the fundamental parameters of the open clusters NGC 189, NGC 1758, and NGC 7762. We followed the processes outlined in Yontan (2023). Dense stellar regions, different membership selection criteria, high/differential extinction towards the cluster regions, and different analyses procedures can influence the determination of the fundamental astrophysical parameters of clusters and result in degeneracies between reddening and age parameters (Anders et al., 2004; King et al., 2005). Such a situation is the cause of large discrepancies across the estimated parameters performed by various researchers for the same clusters. To avoid possible degeneracy issues and achieve accurate calculations, the color excesses and metallicities of the clusters were derived using $(U - B) \times (B - V)$ two-color diagrams (TCDs) separately, while we obtained distance moduli and ages individually by fitting theoretical models on CMDs.

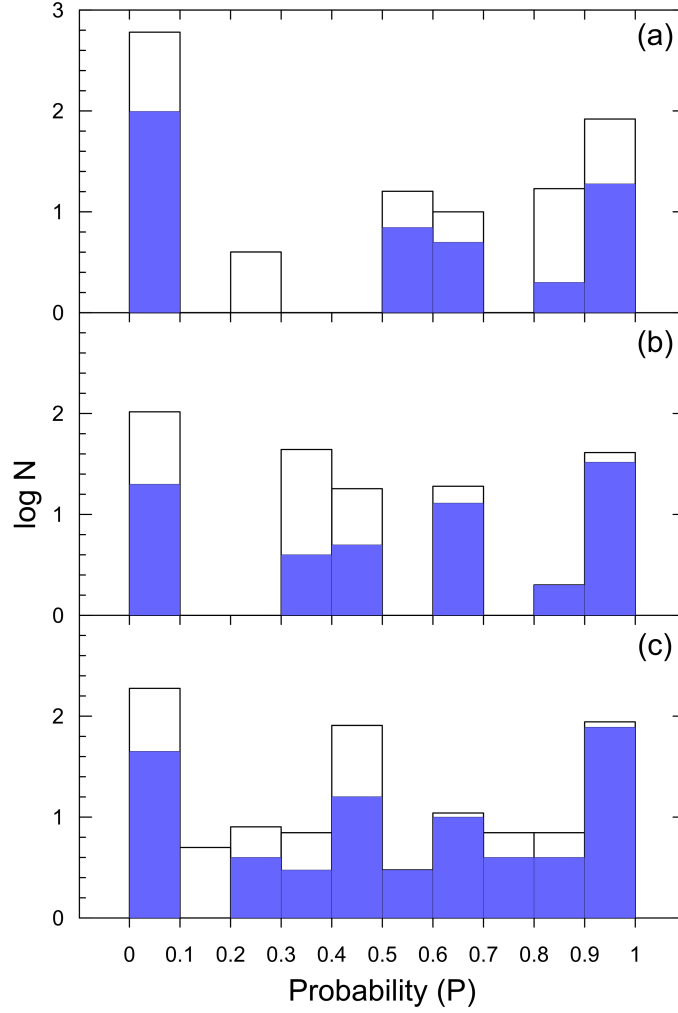


Fig. 5. Histogram of the membership probabilities for the stars in the NGC 189 (a), NGC 1758 (b), and NGC 7762 (c) open clusters. The white shading presents the stars that are detected in the cluster areas, while the purple colored shading denotes the stars that lie within fitted ZAMS lines.

3.1. Color Excess

Estimation of reddening was performed using $(U - B) \times (B - V)$ TCDs of the clusters. We selected the main-sequence member stars with probability $P \geq 0.5$ and within the magnitude ranges $13 \leq V \leq 19$ for NGC 189, $10 \leq V \leq 17$ mag for NGC 1758 and $14 \leq V \leq 17$ mag for NGC 7762 in order to derive the $E(U - B)$ and $E(B - V)$ color excess values. We plotted $(U - B) \times (B - V)$ TCDs using these member stars and fitted the ZAMS of Sung et al. (2013) to these distributions. The ZAMS was fitted by considering varied values of the reddening slope $\alpha = E(U - B)/E(B - V)$, applying a χ^2 minimization method. The best result of minimum χ^2 equates to the reddening slope being $\alpha = 0.72$ as well as the color excess $E(B - V)$ being 0.590 ± 0.023 mag for NGC 189 and 0.310 ± 0.022 mag for NGC 1758. In the case of NGC 7762 the best reddening slope and color excess values are $\alpha = 0.68$ and $E(B - V) = 0.640 \pm 0.017$ mag, respectively. TCDs with the best solutions are presented in Fig. 8. Color excess errors are $\pm 1\sigma$ deviations. Our estimated color excess $E(B - V)$ for NGC 189 is close to the values found by Kharchenko et al. (2013), Joshi et al. (2016) and Dias et al. (2021). For NGC 1758, the estimated $E(B - V)$ is compatible with the studies of Kharchenko et al. (2005) and Sampedro et al. (2017). For NGC 7762 the current estimate is in good agreement with results given by Kharchenko et al. (2013), Maciejewski & Niedzielski (2007) and Cantat-Gaudin et al. (2020). See Table 1 for a detailed comparison.

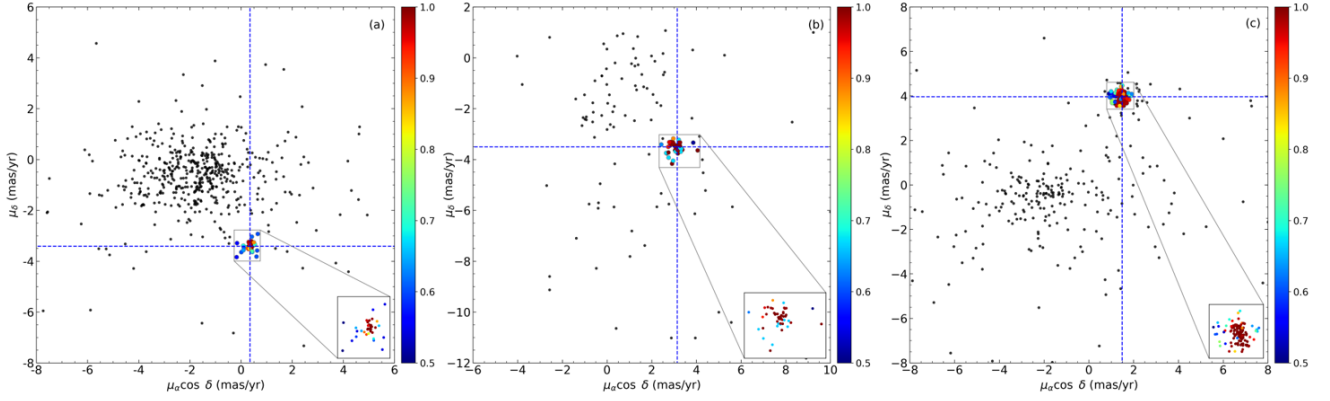


Fig. 6. VPDs of NGC 189 (a), NGC 1758 (b), and NGC 7762 (c) based on *Gaia* DR3 astrometry. The membership probabilities of the stars are identified with the color scale shown on the right for each cluster. The zoomed boxes in panels (a), (b) and (c) represent the region of condensation for each cluster in the VPDs. The mean proper motion value of the clusters is shown with the intersection of the dashed blue lines.

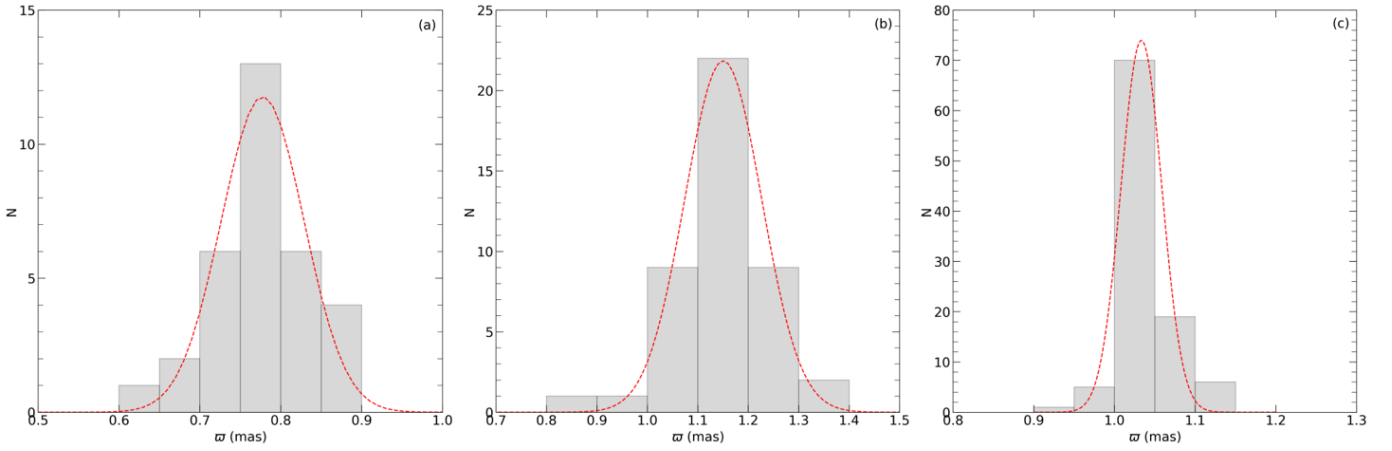


Fig. 7. Histograms of mean trigonometric parallax estimation of NGC 189 (a), NGC 1758 (b), and NGC 7762 (c) from the most probable members ($P \geq 0.50$). Red dashed lines show the fitted Gaussian functions.

3.2. Photometric Metallicities

As with reddening, it is important to know the metallicity before attempting to derive the age and distance of a cluster. Given a lack of spectroscopic observations, $(U - B) \times (B - V)$ TCDs can be used to estimate photometric metallicity (Karaali et al., 2003a,b, 2011). In the present study, we used the method of Karaali et al. (2011) to determine the photometric metallicity of each cluster. In this method, F and G-type main-sequence stars falling into the $0.3 \leq (B - V)_0 \leq 0.6$ mag color range (Eker et al., 2018, 2020) and their UV-excesses are used. Having calculated de-reddened $(B - V)_0$ and $(U - B)_0$ color indices of the most probable member stars ($P \geq 0.5$) and considering the $E(U - B)$, $E(B - V)$ color excesses derived in the study (see Section 3.1), we made a selection of F-G type main-sequence stars by limiting their color range within $0.3 \leq (B - V)_0 \leq 0.6$ mag. This resulted in the selection

Table 5. The median astrometric parameters of the three open clusters. Proper motion components ($\langle \mu_\alpha \cos \delta \rangle$, $\langle \mu_\delta \rangle$), trigonometric parallaxes ($\langle \varpi \rangle$), and the distances (d_ϖ) calculated from the trigonometric parallaxes of the cluster's most probable member stars ($P \geq 0.50$).

Cluster	$\langle \mu_\alpha \cos \delta \rangle$ (mas yr ⁻¹)	$\langle \mu_\delta \rangle$ (mas yr ⁻¹)	$\langle \varpi \rangle$ (mas)	d_ϖ (pc)
NGC 189	+0.352±0.032	-3.412±0.038	0.778±0.051	1285±84
NGC 1758	+3.141±0.035	-3.507±0.025	1.150±0.076	870±57
NGC 7762	+1.489±0.023	+3.962±0.024	1.033±0.025	968±23

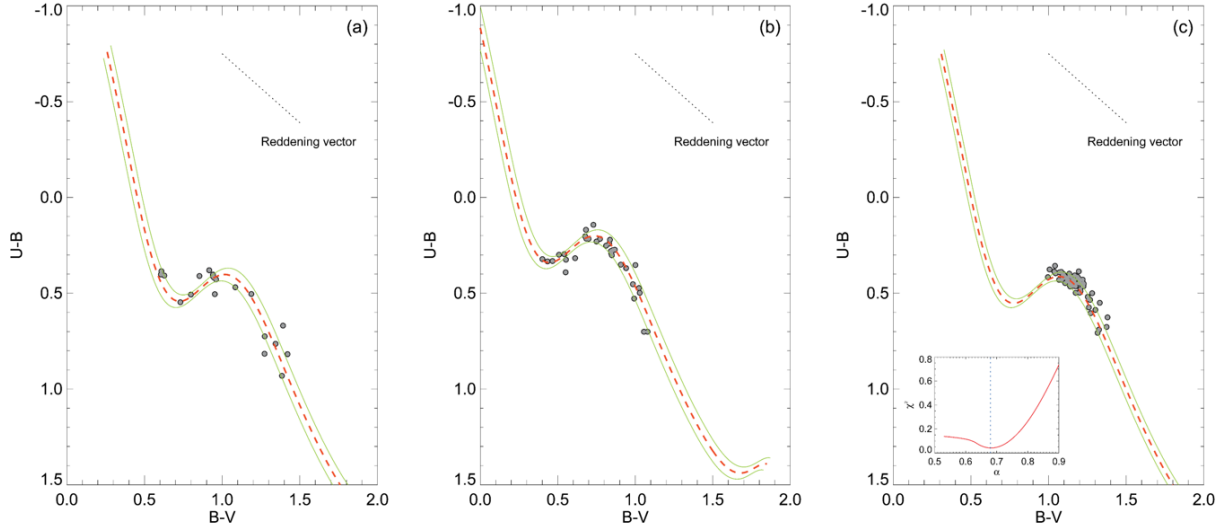


Fig. 8. $(U - B) \times (B - V)$ diagrams with the best-fitted ZAMS for NGC 189 (a), NGC 1758 (b) and NGC 7762 (c). Green-filled circles represent the main-sequence members with the probability $P \geq 0.5$. Red dashed and green solid curves show the reddened ZAMS of Sung et al. (2013) and $\pm 1\sigma$ standard deviations, respectively. In the inner panel of NGC 7762 (panel c), χ^2 values versus the estimated reddening slope are presented. The dashed blue line is the best reddening slope based on χ^2_{\min} .

of five stars for NGC 189, four stars for NGC 1758 and 37 stars for NGC 7762. Next, the construction of $(U - B)_0 \times (B - V)_0$ diagrams (Figure 9 upper panels) was made for these selected stars and compared against that of the Hyades main sequence. This allowed the determination of the differences between the $(U - B)_0$ color indices of the observed cluster members and the Hyades stars which have the same $(B - V)_0$ colors. The calculated $(U - B)_0$ differences are defined as the UV-excess (δ) via the equation $\delta = (U - B)_{0,H} - (U - B)_{0,S}$, where H and S are Hyades and cluster stars, respectively. The calculated UV-excesses were calibrated to the normalised $\delta_{0.6}$ values according to $(B - V)_0 = 0.6$ mag. We plotted histograms of the normalised $\delta_{0.6}$ values and applied Gaussian fits to these distributions to estimate the mean $\delta_{0.6}$ values (Figure 9 lower panels). Considering the peaks of the fitted Gaussian functions, the photometric metallicities of the three open clusters were estimated using the following equation from Karaali et al. (2011):

$$[\text{Fe}/\text{H}] = -14.316(1.919)\delta_{0.6}^2 - 3.557(0.285)\delta_{0.6} + 0.105(0.039). \quad (3)$$

Fig. 9 presents the TCDs and the distributions of the normalised $\delta_{0.6}$ UV excesses for three clusters. The calculated mean $\delta_{0.6}$ values of NGC 189, NGC 1758, and NGC 7762 are 0.044 ± 0.014 mag, 0.044 ± 0.011 mag, and 0.053 ± 0.019 mag respectively. Thus, the estimated photometric metallicities are $[\text{Fe}/\text{H}] = -0.08 \pm 0.03$ dex for NGC 189, $[\text{Fe}/\text{H}] = -0.08 \pm 0.03$ dex for NGC 1758 and $[\text{Fe}/\text{H}] = -0.12 \pm 0.02$ dex for NGC 7762. Moreover, estimated photometric metallicities ($[\text{Fe}/\text{H}]$) were converted to the mass fraction z for choosing isochrones used in age determination. To do this, we took into account the expressions presented from Bovy⁴ which are improved for PARSEC isochrones (Bressan et al., 2012). The related expressions are given as follows:

$$z_x = 10^{[\text{Fe}/\text{H}] + \log\left(\frac{z_0}{1 - 0.248 - 2.78 \times z_0}\right)} \quad (4)$$

and

$$z = \frac{(z_x - 0.2485 \times z_x)}{(2.78 \times z_x + 1)}. \quad (5)$$

⁴<https://github.com/jobovy/isodist/blob/master/isodist/Isochrone.py>

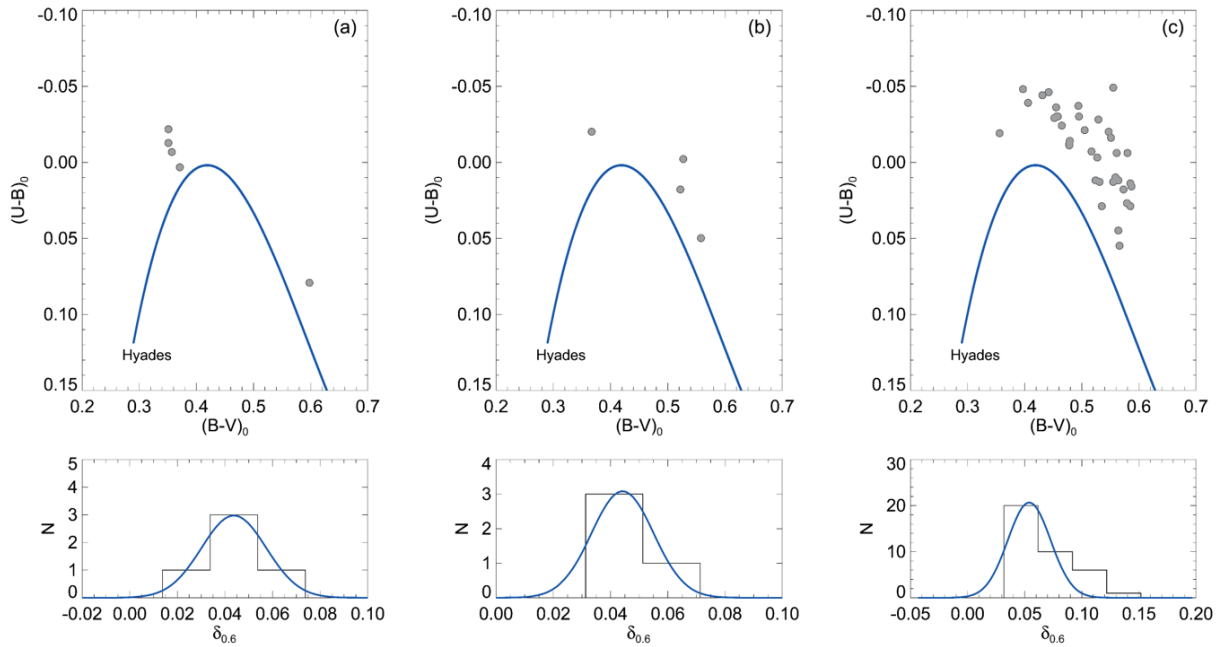


Fig. 9. $(U - B)_0 \times (B - V)_0$ diagrams (upper panels) and histograms for the normalized $\delta_{0,6}$ (lower panels) for five stars (NGC 189, panel a), four stars (NGC 1758, panel b), and 37 stars (NGC 7762, panel c) F-G type main-sequence stars with probability $P \geq 0.5$. The solid blue lines in the upper panels represent the main sequence of Hyades, whereas Gaussian fits in the lower panels.

Where z_x and z_\odot are intermediate values where solar metallicity z_\odot was adopted as 0.0152 (Bressan et al., 2012). We obtained $z = 0.013$ for NGC 189 and NGC 1758 as well as $z = 0.012$ for NGC 7762.

3.3. Distance and Age

In the present study, the age and distance moduli of the studied clusters were estimated simultaneously by fitting PARSEC isochrones (Bressan et al., 2012) to the observed CMDs. We plotted $V \times (U - B)$, $V \times (B - V)$ and $G \times (G_{BP} - G_{RP})$ CMDs and fitted selected isochrones via visual inspection, taking into account the main-sequence, turn-off, and giant stars with membership probabilities $P \geq 0.5$. For each cluster, selection of PARSEC isochrones⁵ was made according to the mass fraction z calculated from photometric metallicities earlier in this study (Section 3.2). For the UBV data-driven isochrone fitting process, the isochrones were reddened in regard to the color excesses $E(U - B)$ and $E(B - V)$ as determined in this study, while the *Gaia* DR3 reddened procedure employed the equation $E(G_{BP} - G_{RP}) = 1.41 \times E(B - V)$ as given by Sun et al. (2021). Errors for distance moduli and distances were obtained from the expression presented by Carraro et al. (2017). Uncertainties in age were estimated by considering the scatter of the observed data representing the main sequence, turn off and giant member stars. We, therefore, selected low and high-age isochrones whose values were close to the cluster's estimated age, taking into account this scatter. $V \times (U - B)$, $V \times (B - V)$ and $G \times (G_{BP} - G_{RP})$ CMDs with the best fitting isochrones are given as Fig. 10. Estimated distance moduli and ages for each cluster are as follows:

- **NGC 189:** We over-plotted the different isochrones of $\log(\text{age}) = 8.65, 8.70$ and 8.74 with $z = 0.013$ on all the CMDs for the cluster NGC 189, as shown in Fig. 10 (panels a, b and c). The age of NGC 189 is estimated from the well-fitting isochrone $\log(\text{age}) = 8.70$ log-years to the most probable main-sequence and giant stars, and corresponds to the age $t = 500 \pm 50$ Myr.

⁵<http://stev.oapd.inaf.it/cgi-bin/cmd>

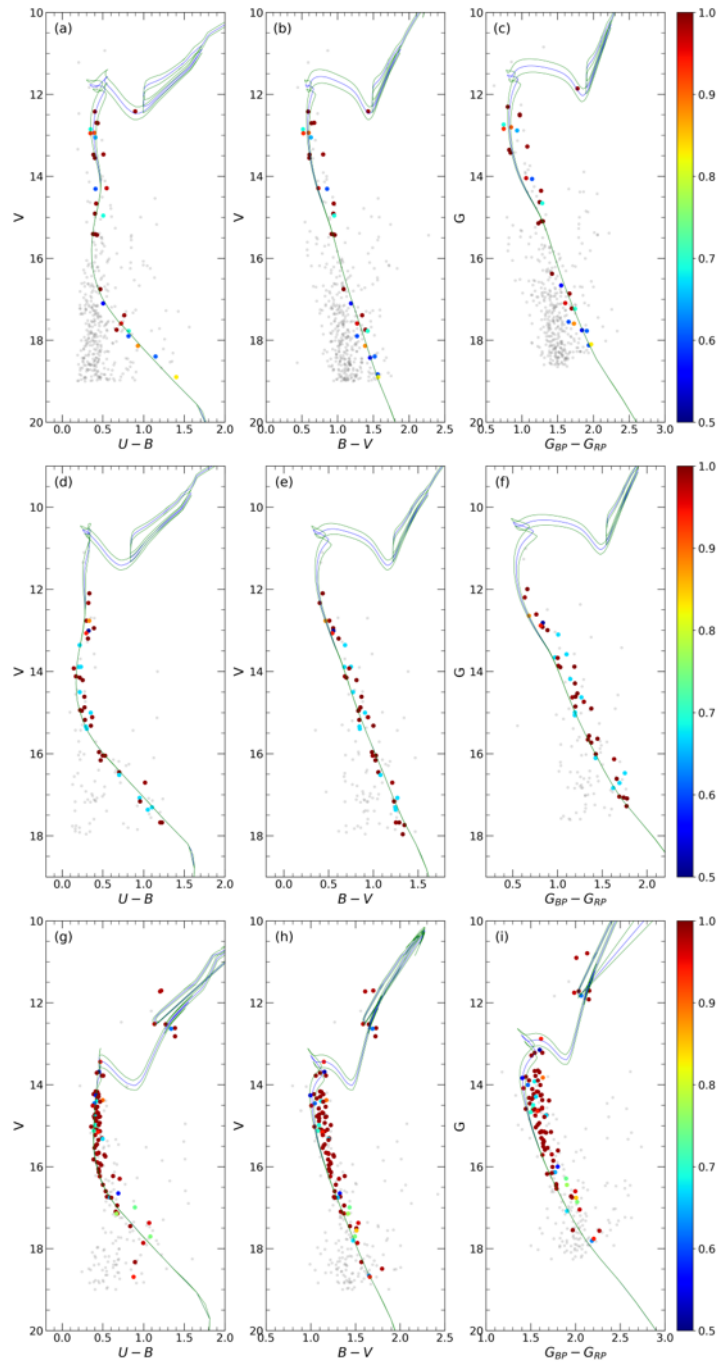


Fig. 10. Color-magnitude diagrams for the studied clusters NGC 189 (panels a, b and c), NGC 1758 (panels d, e and f) and NGC 7762 (panels g, h and i). Different color correspond to the membership probabilities of the most probable cluster members. The scales of membership probabilities are represented on color bars to the right of the figure. Grey colored dots identify the stars with probabilities $P < 0.5$. The best fitting PARSEC isochrones and their errors are shown as the blue lines and green dashed lines, respectively. Superimposed isochrone ages match to 500 Myr for NGC 189, 650 Myr for NGC 1758 and 2000 Myr for NGC 7762.

The derived age is in good agreement with the results of Kharchenko et al. (2013), Joshi et al. (2016) and Loktin & Popova (2017). We derived the distance modulus of the NGC 189 as $\mu_V = 12.227 \pm 0.094$ mag, which leads to the isochrones-based distance for the cluster being $d_{\text{iso}} = 1201 \pm 53$ pc. This distance value is close to most of the values given by many authors (etc. Cantat-Gaudin et al., 2018, 2020, see Table 1 for detailed comparison). The isochrone distance estimated for the cluster is compatible with the astrometric distance value ($d_{\pi} = 1285 \pm 84$ pc) calculated from *Gaia* DR3 trigonometric parallaxes of member stars. We estimated the Galactocentric distance as $R_{\text{gc}} = 8.69$ kpc by considering the Sun's distance to the Galactic centre as 8 kpc (Majewski, 1993). The Galactocentric coordinates were derived as $(X, Y, Z)_{\odot} = (-627, 1024, -36)$ pc, respectively. These are compatible with the values of Cantat-Gaudin et al. (2018).

- **NGC 1758:** We over-plotted the isochrones $\log(\text{age}) = 8.78, 8.81$ and 8.84 with $z = 0.013$ to the observed CMDs as presented in Fig. 10 (panels d, e and f). The best-fit isochrone corresponded to the age of the NGC 1758 being $\log(\text{age}) = 8.70$ or a value of $t = 650 \pm 50$ Myr. This age estimate is about 100 Myr older than the estimated ages presented by Bossini et al. (2019) and Dias et al. (2021). We estimated the distance modulus of the NGC 1758 as $\mu_V = 10.736 \pm 0.078$ mag. This corresponds to the isochrone-based distance for the cluster being $d_{\text{iso}} = 902 \pm 33$ pc. This result is close to the values given by Liu & Pang (2019) and Bossini et al. (2019). It is also compatible with the results given by Cantat-Gaudin et al. (2018), Cantat-Gaudin & Anders (2020), and Dias et al. (2021) (see Table 1 for a detailed comparison). The isochrone distance estimated for the NGC 1758 is compatible with the astrometric distance value of $d_{\pi} = 870 \pm 57$ pc. The Galactocentric distance and Galactocentric coordinates were obtained as $R_{\text{gc}} = 8.89$ kpc and $(X, Y, Z)_{\odot} = (-887, 13, -164)$ pc. These are in good agreement with the values of Cantat-Gaudin et al. (2018).
- **NGC 7762:** Isochrones of ages $\log(\text{age}) = 9.25, 9.30$ and 9.35 were over-plotted with $z = 0.012$ to the *UBV* and *Gaia* data-based CMDs, as shown in Fig. 10 (panels g, h and i). Considering the most probable main sequence, turn-off and giant cluster members, we concluded that the best fitting isochrone gives the age of the NGC 7762 as $\log(\text{age}) = 9.30$, which corresponds to $t = 2000 \pm 200$ Myr. The estimated age of the cluster is in good agreement with the values of Maciejewski & Niedzielski (2007), Joshi et al. (2016) and Cantat-Gaudin et al. (2020). We obtained the distance modulus of the NGC 7762 as $\mu_V = 11.781 \pm 0.072$ mag, which gives the isochrone-based distance of the cluster as $d_{\text{iso}} = 911 \pm 31$ pc. This value is compatible with the values given in many studies which are based on *Gaia* data (Soubiran et al., 2018; Cantat-Gaudin et al., 2020; Cantat-Gaudin & Anders, 2020, see Table 1 for a detailed comparison). The isochrone distance is close to the distance value ($d_{\pi} = 968 \pm 23$ pc) calculated from *Gaia* DR3 trigonometric parallaxes in this study. The Galactocentric distance and Galactocentric coordinates were obtained as $R_{\text{gc}} = 8.45$ kpc and $(X, Y, Z)_{\odot} = (-414, 806, 93)$ pc. These are compatible with the corresponding estimates of Cantat-Gaudin et al. (2018).

4. Kinematics and Galactic orbit parameters

We estimated the space velocity components and Galactic orbit parameters of NGC 189, NGC 1758 and NGC 7762 using the Python package *GALPY* Bovy (2015)⁶. To perform integrations of the Galactic orbits for these clusters, we adopted the default *GALPY* potential of the Milky Way that assumes an axisymmetric potential for the Galaxy (MWPOTENTIAL2014, Bovy 2015). The

⁶See also <https://galpy.readthedocs.io/en/v1.5.0/>

MILKYWAYPOTENTIAL2014 code is described by a three-component model consisting of the bulge, disc, and halo potentials. The bulge is described as a spherical power-law density profile according to the expression of Bovy (2015):

$$\rho(r) = A \left(\frac{r_1}{r} \right)^\alpha \exp \left[- \left(\frac{r}{r_c} \right)^2 \right] \quad (6)$$

where r_1 and r_c are the present reference radius and cut-off radius, respectively. A and α denote the amplitude that is applied to the potential in mass density units and inner power, respectively. The Galactic disc component that we used is expressed by Miyamoto & Nagai (1975) as:

$$\Phi_{\text{disc}}(R_{\text{gc}}, Z) = - \frac{GM_d}{\sqrt{R_{\text{gc}}^2 + \left(a_d + \sqrt{Z^2 + b_d^2} \right)^2}} \quad (7)$$

where R_{gc} and Z are the distances from the Galactic centre and Galactic plane, respectively. G is the universal gravitational constant, and M_d the mass of the Galactic disc, a_d the scale length of the disc and b_d the height of the disc. The halo component is assumed as a spherically symmetric spatial distribution of the dark matter density. The expression of Navarro et al. (1996) was adopted to model the halo as:

$$\Phi_{\text{halo}}(r) = - \frac{GM_s}{R_{\text{gc}}} \ln \left(1 + \frac{R_{\text{gc}}}{r_s} \right) \quad (8)$$

where M_s denotes the mass of the dark matter halo of the Milky Way and r_s represents its radius. The galactocentric distance and the circular velocity of the Sun were taken as $R_{\text{gc}} = 8$ kpc and $V_{\text{rot}} = 220$ km s⁻¹, respectively (Bovy & Tremaine, 2012; Bovy, 2015). The Sun's distance from the Galactic plane was taken as 27 ± 4 pc (Chen et al., 2001).

The input parameters for the orbital integration of the three clusters are listed in Table 6, namely the equatorial coordinates (α , δ) estimated in the study (Section 2.3), proper motion components ($\mu_\alpha \cos \delta$, μ_δ) estimated in Section 2.4, distance (d_{iso}) from the Section 3.3, and radial velocity (V_r). The radial velocities of the clusters were derived using the data available in the *Gaia* DR3 catalogue. To calculate the mean radial velocities (and their uncertainties) of the clusters, we selected the stars with membership probabilities $P \geq 0.9$ and used the weighted average of their radial velocities taken from *Gaia* DR3 data (for equations see Soubiran et al., 2018). The mean radial velocities were calculated as -29.60 ± 0.32 km s⁻¹ for NGC 189 from five member stars, as $+6.80 \pm 2.90$ km s⁻¹ for NGC 1758 from eight members, and -46.61 ± 0.10 km s⁻¹ for NGC 7762 from 31 members. The literature mean radial velocity estimates for NGC 189 are -28.47 ± 0.75 (Soubiran et al., 2018) and -29.391 ± 0.534 km s⁻¹ (Dias et al., 2021), while for NGC 1758 the literature value is 17.840 ± 9.887 km s⁻¹ (Dias et al., 2021). The values for NGC 7762 are -45.7 ± 0.7 km s⁻¹ (Casamiquela et al., 2016), -45.40 ± 0.14 km s⁻¹ (Soubiran et al., 2018) and -45.438 ± 0.492 km s⁻¹ (Dias et al., 2021) (Table 1). The mean radial velocities derived in this study for NGC 189 and NGC 7762 are within 1-2 km s⁻¹ of the values given by these different researchers. In the case of NGC 1758, there is a difference between the estimated and literature mean radial velocity value. We used radial velocities of eight stars with membership probabilities $P \geq 0.9$ for NGC 1758, whereas in the study of Dias et al. (2021) the mean radial velocity of the cluster was estimated from two members. We concluded that the reason for the discrepancies between these two studies is the number and membership probabilities of the stars used in calculations.

Kinematic and dynamic calculations were analyzed with 1 Myr steps over a 3 Gyr integration time. Estimates for the apogalactic distance R_a , perigalactic distance R_p , eccentricity e , the maximum vertical distance from Galactic plane Z_{max} , Galactic space velocity components (U , V , W), and orbital period P_{orb} were derived and listed in Table 6. The space velocity components (U , V , W) were estimated as $(14.83 \pm 0.37, -26.31 \pm 0.12, -18.59 \pm 0.78)$ km s⁻¹ for NGC 189, $(-7.38 \pm 2.91, -19.91 \pm 0.78, 0.71 \pm 0.28)$ km s⁻¹

for NGC 1758 and $(12.73 \pm 0.50, -47.32 \pm 0.23, 10.27 \pm 0.71)$ km s⁻¹ for NGC 7762. To apply the local standard of rest (LSR), we employed the velocity components of Coşkunoğlu et al. (2011) as $(U, V, W) = (8.83 \pm 0.24, 14.19 \pm 0.34, 6.57 \pm 0.21)$ km s⁻¹. Hence, we derived transformed parameters $(U, V, W)_{\text{LSR}}$ as $(23.66 \pm 0.44, -12.12 \pm 0.36, -12.02 \pm 0.80)$ km s⁻¹ for NGC 189, $(1.46 \pm 2.92, -5.72 \pm 0.85, 7.28 \pm 0.35)$ km s⁻¹ for NGC 1758 and $(21.56 \pm 0.56, -33.13 \pm 0.41, 16.84 \pm 0.74)$ km s⁻¹ for NGC 7762. Moreover, the total space velocities (S_{LSR}) of NGC 189 were calculated to be 29.17 ± 0.98 km s⁻¹, 9.37 ± 3.06 km s⁻¹ for NGC 1758 and 42.96 ± 1.02 km s⁻¹ for NGC 1798 (for all estimated parameters see Table 6). To obtain the birth radii of three clusters, we utilized the orbital integration in the past epochs, using time bins equal to estimated cluster ages.

The Galactic orbits of the three clusters are represented in Fig. 11. The left panels of this figure show the ‘side views’ of the cluster motions (panel a for NGC 189; panel c for NGC 1758 and panel e for NGC 7762) in respect of distance from the Galactic center and the Galactic plane. According to the analyses, both NGC 189 and NGC 1758 follow a ‘boxy’ pattern with almost zero eccentricities, whereas the orbit of the NGC 7762 differs from a ‘boxy’ pattern given its larger eccentricity. We investigated the orbital parameters to understand how uncertainties in the input parameters ($\mu_\alpha \cos \delta, \mu_\delta, d_{\text{iso}}$, and V_γ) influence the orbit integration results and estimated birth-radii of the clusters. In the right panel of the Fig. 11 the motion in the Galactic disc and the effect of uncertainties in the input parameters are presented in terms of time for the three clusters (panel b for NGC 189; panel d for NGC 1758, and panel f for NGC 7762). It can be seen from the figure that the range in possible birth radii, between the extreme estimates, do not exceed 0.4 kpc for any of the three clusters.

These estimates for the birth-radii indicate that both NGC 189 and NGC 1758 were formed outside the solar vicinity at 8.58 and 8.42 kpc, while NGC 7762 was formed inside the solar vicinity with a birth radius of 6.70 kpc. According to the perigalactic and apogalactic distances of the three clusters, it can be concluded that the orbit of NGC 1758 is completely outside the solar circle (Fig. 11e), while NGC 189 and NGC 7762 cross the solar circle during their orbits (Fig. 11a and c, respectively). All three clusters rise above the plane up to $Z_{\text{max}} = 310$ pc. This indicates that NGC 189, NGC 1758 and NGC 7762 belong to the thin-disc component of the Milky Way (Bilir et al., 2006b,c, 2008).

5. Summary & Conclusions

We presented photometric, astrometric, and kinematic studies of the open clusters NGC 189, NGC 1758 and NGC 7762 using CCD *UBV* and *Gaia* DR3 data. We identified 32, 57 and 106 member stars (with estimated membership probabilities $P \geq 0.5$) in the regions of NGC 189, NGC 1758, and NGC 7762, respectively. These members were employed in the estimation of the main astrophysical parameters of the clusters. We used *UBV* data-based TCDs, deriving color excesses and photometric metallicities separately to achieve reliable age and distance values. We also investigated the kinematical properties of the clusters. The results of these analyses are listed in Table 6. In literature studies, parameters were derived simultaneously through statistical solutions for the three clusters. This can cause degeneracies between the parameters (reddening, age and distance) and large uncertainties in the measured values. We therefore believe that the approach described in this paper leads to more reliable estimates.

The main findings of the current study are summarized as follows:

1. We investigated the structural properties of the clusters. We used the central coordinates determined in the study during RDP analyses. The centers of three clusters are:
 - ($\alpha = 00^{\text{h}}39^{\text{m}}27^{\text{s}}.89, \delta = +61^{\circ}06'46''.35$) for NGC 189,
 - ($\alpha = 05^{\text{h}}04^{\text{m}}42^{\text{s}}.00, \delta = +23^{\circ}48'46''.90$) for NGC 1758, and

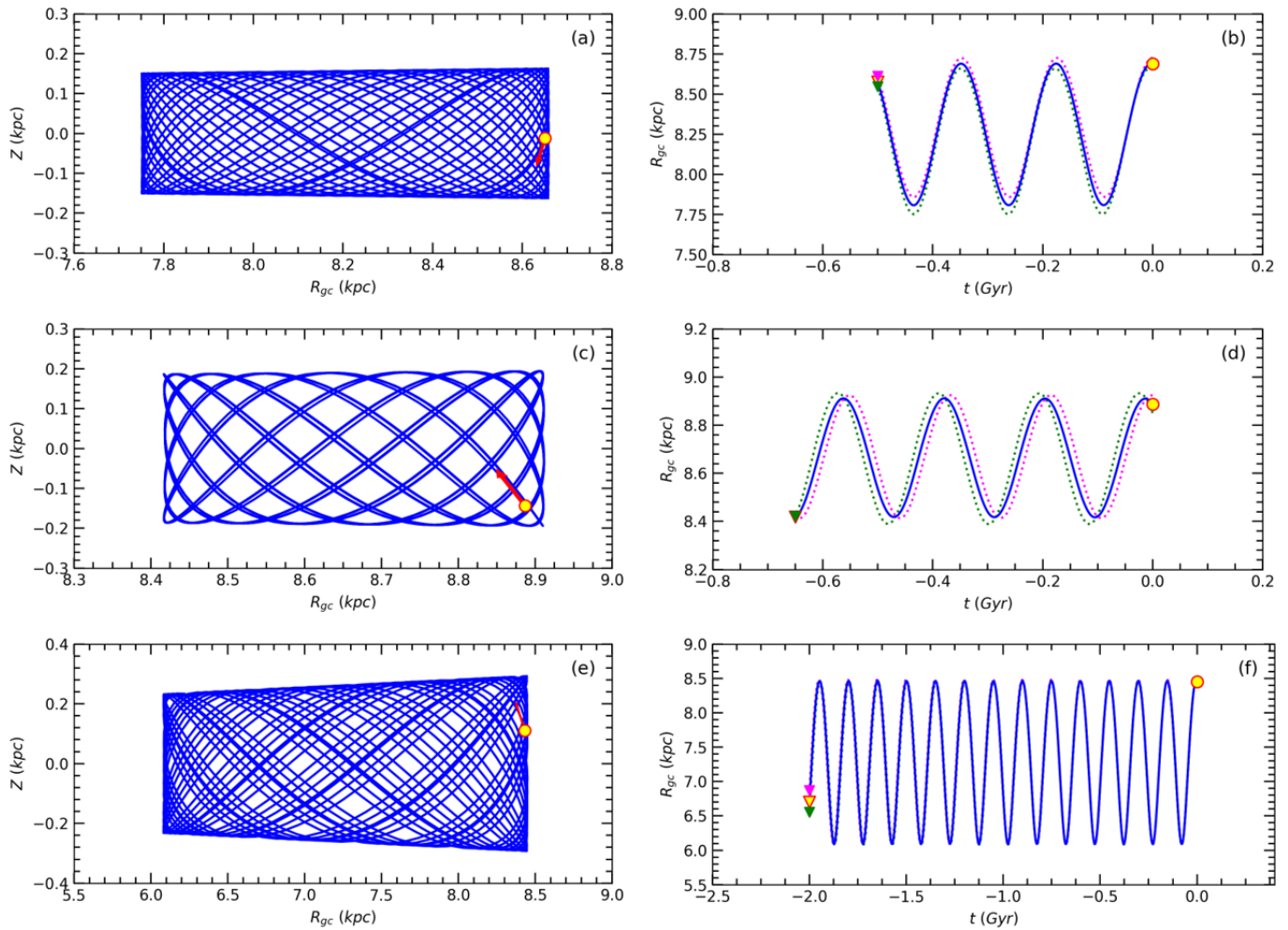


Fig. 11. The Galactic orbits and birth radii of NGC 189 (a, b), NGC 1758 (c, d) and NGC 7762 (e, f) in the $Z \times R_{gc}$ and $R_{gc} \times t$ planes. The filled yellow circles and triangles show the present-day and birth positions, respectively. Red arrows are the motion vectors of open clusters. The green and pink dotted lines show the orbit when errors in input parameters are considered, while the green and pink filled triangles represent the birth locations of the open cluster based on the lower and upper error estimates.

Table 6. Fundamental parameters of NGC 189, NGC 1758 and NGC 7762.

Parameter	NGC 189	NGC 1758	NGC 7762
$(\alpha, \delta)_{J2000}$ (Sexagesimal)	00:39:27.89, +61:06:46.35	05:04:42.00, +23:48:46.90	23:49:53.00, +68:02:06.00
$(l, b)_{J2000}$ (Decimal)	121.4858, -01.7252	179.1584, -10.4597	117.2060, +05.8501
f_0 (stars arcmin ⁻²)	4.86 ± 0.41	2.97 ± 0.17	4.91 ± 0.24
f_{bg} (stars arcmin ⁻²)	12.38 ± 0.08	3.14 ± 0.08	4.92 ± 0.13
r_c (arcmin)	0.81 ± 0.12	2.13 ± 0.28	4.39 ± 0.46
r_{lim} (arcmin)	4	7	15
r (pc)	1.40	1.98	3.97
Cluster members ($P \geq 0.5$)	32	57	106
$\mu_\alpha \cos \delta$ (mas yr ⁻¹)	0.352 ± 0.032	3.141 ± 0.035	1.489 ± 0.023
μ_δ (mas yr ⁻¹)	-3.412 ± 0.038	-3.507 ± 0.025	3.962 ± 0.024
ϖ (mas)	0.778 ± 0.051	1.150 ± 0.076	1.033 ± 0.025
d_ϖ (pc)	1285 ± 84	870 ± 57	968 ± 23
$E(B - V)$ (mag)	0.590 ± 0.023	0.310 ± 0.022	0.640 ± 0.017
$E(U - B)$ (mag)	0.425 ± 0.017	0.223 ± 0.016	0.435 ± 0.012
A_V (mag)	1.829 ± 0.071	0.961 ± 0.068	1.984 ± 0.053
$E(G_{BP} - G_{RP})$ (mag)	0.832 ± 0.032	0.437 ± 0.031	0.902 ± 0.024
A_G (mag)	1.548 ± 0.026	0.814 ± 0.047	1.680 ± 0.039
[Fe/H] (dex)	-0.08 ± 0.03	-0.08 ± 0.03	-0.12 ± 0.02
Age (Myr)	500 ± 50	650 ± 50	2000 ± 200
Distance modulus (mag)	12.227 ± 0.094	10.736 ± 0.078	11.781 ± 0.072
Isochrone distance (pc)	1201 ± 53	902 ± 33	911 ± 31
$(X, Y, Z)_\odot$ (pc)	(-627, 1024, -36)	(-887, 13, -164)	(-414, 806, 93)
R_{gc} (kpc)	8.69	8.89	8.45
V_γ (km/s)	-29.60 ± 0.32	6.80 ± 2.90	-46.61 ± 0.10
U_{LSR} (km/s)	23.66 ± 0.44	1.46 ± 2.92	21.56 ± 0.56
V_{LSR} (km/s)	-12.12 ± 0.36	-5.72 ± 0.85	-33.13 ± 0.41
W_{LSR} (km/s)	-12.02 ± 0.80	7.28 ± 0.35	16.84 ± 0.74
S_{LSR} (km/s)	29.17 ± 0.98	9.37 ± 3.06	42.96 ± 1.02
R_a (pc)	8690 ± 36	8912 ± 22	8466 ± 17
R_p (pc)	7808 ± 56	8418 ± 28	6091 ± 7
z_{max} (pc)	177 ± 14	194 ± 3	307 ± 16
e	0.053 ± 0.002	0.029 ± 0.003	0.163 ± 0.001
P_{orb} (Myr)	231 ± 2	244 ± 1	203 ± 1
Birthplace (kpc)	8.58	8.42	6.70

- ($\alpha = 23^{\text{h}}49^{\text{m}}53^{\text{s}}.00, \delta = +68^{\circ}02'06''.00$) for NGC 7762.

The limiting radii r_{lim} were obtained as 4' for NGC 189, 7' for NGC 1758, and 15' for NGC 7762. Astrometric analyzes showed that NGC 1746 does not exist, but has been misidentified in the past and instead is NGC 1758.

2. We separated cluster members from the field stars by considering *UBV* data-based CMDs as well as the *Gaia* DR3 proper motion and trigonometric parallax data. We utilized the *UPMASK* method to calculate the membership probabilities of stars. Based on the distribution of the most probable member stars ($P \geq 0.5$) on $V \times (B - V)$ CMDs, we fitted ZAMS curves that included the effect of possible binary star contamination on the cluster main sequence. From the location of these selected stars on VPDs, we derived mean proper motion components as:

- $(-0.352 \pm 0.032, -3.412 \pm 0.038)$ mas yr⁻¹ for NGC 189,
- $(3.141 \pm 0.035, -3.507 \pm 0.025)$ mas yr⁻¹ for NGC 1758 and
- $(1.489 \pm 0.023, 3.962 \pm 0.024)$ mas yr⁻¹ for NGC 7762.

Utilizing the Gaussian fits on histograms constructed from most probable member stars' *Gaia* DR3 trigonometric parallaxes (ϖ), we determined mean trigonometric parallaxes as 0.778 ± 0.051 mas for NGC 189, 1.150 ± 0.076 mas for NGC 1758 and 1.033 ± 0.025 mas for NGC 7762. Using the equation $d(\text{pc}) = 1000/\varpi$ (mas), we converted the mean trigonometric values into astrometric distances (d_{ϖ}):

- 1285 ± 84 pc for NGC 189,
- 870 ± 57 pc for NGC 1758 and
- 968 ± 23 pc for NGC 7762.

3. Comparison of the $(U - B) \times (B - V)$ diagrams of most probable member stars with the ZAMS (Sung et al., 2013) via χ^2 minimization led to estimates of the reddening slope $\alpha = E(U - B)/E(B - V)$ and color excesses $E(B - V)$ for the clusters. The best fitting solutions corresponded to $\alpha = 0.72$ and $E(B - V) = 0.590 \pm 0.023$ mag for NGC 189, 0.72 and 0.310 ± 0.022 mag for NGC 1758 and 0.68 and 0.640 ± 0.017 mag for NGC 7762.
4. Estimation of photometric metallicity is based on the calculation of UV-excesses of selected F-G main-sequence stars with membership probabilities $P \geq 0.5$, compared to the Hyades main-sequence on $(U - B) \times (B - V)$ diagrams. The values of photometric metallicities ([Fe/H]) were calculated as -0.08 ± 0.03 dex for NGC 189, -0.08 ± 0.03 dex for NGC 1758 and -0.12 ± 0.02 dex for NGC 7762. We transformed the [Fe/H] values to mass fractions z to derive the ages and distances of the clusters (in the following step below). These are $z = 0.013$ for NGC 189 and NGC 1758, while $z = 0.012$ for NGC 7762.
5. Keeping the color excess and metallicity parameters as constants, we derived distance moduli and ages by fitting *PARSEC* isochrones to the CMDs of the clusters constructed from *UBV* and *Gaia* DR3 data. The distance moduli (μ_V), isochrone distances (d_{iso}), and ages (t) were found to be:
 - 12.227 ± 0.094 mag, 1201 ± 53 pc, 500 ± 50 Myr for NGC 189, respectively;
 - 10.736 ± 0.078 mag, 902 ± 33 pc, and 650 ± 50 Myr for NGC 1758 and
 - 11.781 ± 0.072 mag, 911 ± 31 pc, and 2000 ± 200 Myr for NGC 7762.
6. We calculated the mean radial velocities of the clusters using only the stars with membership probabilities $P \geq 0.9$ and taking into account the radial velocities available in *Gaia* DR3 database. This allowed us to estimate the kinematic properties of the

clusters. The values of the mean radial velocities (V_r) were estimated to be $-29.60 \pm 0.32 \text{ km s}^{-1}$ for NGC 189, $6.80 \pm 2.90 \text{ km s}^{-1}$ for NGC 1758 and $-46.61 \pm 0.10 \text{ km s}^{-1}$ for NGC 7762.

- Galactic orbits and their relevant output parameters were derived using the MWPOTENTIAL2014 of Bovy (2015). We concluded that NGC 189 and NGC 7762 are following ‘boxy’ orbits. Estimates for the birth-radii indicate that both NGC 189 and NGC 1758 were formed outside the solar vicinity at 8.58 and 8.42 kpc, respectively while NGC 7762 was formed inside the solar vicinity with a birth radius of 6.70 kpc.

Acknowledgments

This study has been supported in part by the Scientific and Technological Research Council (TÜBİTAK) 122F109. The observations of this publication were made at the National Astronomical Observatory, San Pedro Mártir, Baja California, México, and the authors wish to thank the staff of the Observatory for their assistance during these observations. This research has made use of the WEBDA database, operated at the Department of Theoretical Physics and Astrophysics of the Masaryk University. We also made use of NASA’s Astrophysics Data System as well as the VizieR and Simbad databases at CDS, Strasbourg, France and data from the European Space Agency (ESA) mission *Gaia*⁷, processed by the *Gaia* Data Processing and Analysis Consortium (DPAC)⁸. Funding for DPAC has been provided by national institutions, in particular the institutions participating in the *Gaia* Multilateral Agreement. IRAF was distributed by the National Optical Astronomy Observatory, which was operated by the Association of Universities for Research in Astronomy (AURA) under a cooperative agreement with the National Science Foundation. PyRAF is a product of the Space Telescope Science Institute, which is operated by AURA for NASA. We thank the University of Queensland for the collaboration software. We are grateful to the anonymous referees for their feedback, which improved the paper.

References

- Adamo, A., Zeidler, P., Kruijssen, J. M. D. et al. (2020). Star clusters near and far. *Space Science Reviews*, 216(4), 69.
- Ak, T., Bostancı, Z. F., Yontan, T. et al. (2016). CCD UBV photometry of the open cluster NGC 6819. *Astrophysics and Space Science*, 361(4), 126. doi:10.1007/s10509-016-2707-2.
- Akbulut, B., Ak, S., Yontan, T. et al. (2021). A study of the Czernik 2 and NGC 7654 open clusters using CCD UBV photometric and Gaia EDR3 data. *Astrophysics and Space Science*, 366(7), 68. doi:10.1007/s10509-021-03975-x.
- Alter, G. (1944). A Photographic Survey of Galactic Clusters: V. NGC 189, I 1590, 358, 366, 381, 433, 436, 457, 609, 637, I 166, 743. *Monthly Notices of the Royal Astronomical Society*, 104(3), 179–190. doi:10.1093/mnras/104.3.179.
- Anders, P., Bissantz, N., Fritze-v. Alvensleben, U. et al. (2004). Analysing observed star cluster SEDs with evolutionary synthesis models: systematic uncertainties. *Monthly Notices of the Royal Astronomical Society*, 347(1), 196–212. doi:10.1111/j.1365-2966.2004.07197.x.
- Balazs, B. A. (1961). Dreifarben-Photometrie von NGC 189 und Stock 24. *Astronomische Abhandlungen der Hamburger Sternwarte*, 5(10), 317–339.
- Banks, T., Yontan, T., Bilir, S. et al. (2020). Vilnius photometry and Gaia astrometry of Melotte 105. *Journal of Astrophysics and Astronomy*, 41(1), 6. doi:10.1007/s12036-020-9621-2.
- Becker, W., & Fenkart, R. (1971). A catalogue of galactic star clusters observed in three colours. *Astronomy and Astrophysics Supplement*, 4(1), 241–252.
- Bilir, S., Bostancı, Z. F., Yontan, T. et al. (2016). CCD UBV photometry and kinematics of the open cluster NGC 225. *Advances in Space Research*, 58(9), 1900–1914. doi:10.1016/j.asr.2016.06.039.
- Bilir, S., Cabrera-Lavers, A., Karaali, S. et al. (2008). Estimation of Galactic Model Parameters in High Latitudes with SDSS. *Publications of the Astronomical Society of Australia*, 25(2), 69–84. doi:10.1071/AS07026.
- Bilir, S., Güver, T., & Aslan, M. (2006a). Separation of dwarf and giant stars with ROTSE-IIIc. *Astronomische Nachrichten*, 327(7), 693. doi:10.1002/asna.200510614.
- Bilir, S., Güver, T., Khamitov, I. et al. (2010). CCD BV and 2MASS photometric study of the open cluster NGC 1513. *Astrophysics and Space Science*, 326(1), 139–150. doi:10.1007/s10509-009-0233-1.
- Bilir, S., Karaali, S., Ak, S. et al. (2006b). Galactic longitude dependent galactic model parameters. *New Astronomy*, 12(3), 234–245. doi:10.1016/j.newast.2006.10.001.
- Bilir, S., Karaali, S., & Gilmore, G. (2006c). Investigation of the ELAIS field by Vega photometry: absolute magnitude-dependent Galactic model parameters. *Monthly Notices of the Royal Astronomical Society*, 366(4), 1295–1309. doi:10.1111/j.1365-2966.2006.09891.x.
- Bisht, D., Zhu, Q., Yadav, R. K. S. et al. (2020). A comprehensive study of open clusters Czernik 14, Haffner 14, Haffner 17 and King 10 using multicolour photometry and Gaia DR2 astrometry. *Monthly Notices of the Royal Astronomical Society*, 494(1), 607–623. doi:10.1093/mnras/staa656.

⁷<https://www.cosmos.esa.int/gaia>

⁸<https://www.cosmos.esa.int/web/gaia/dpac/consortium>

- Bonatto, C., & Bica, E. (2011). From proper motions to star cluster dynamics: measuring the velocity dispersion in deconvolved distribution functions. *Monthly Notices of the Royal Astronomical Society*, 415(1), 313–322. doi:10.1111/j.1365-2966.2011.18699.x.
- Bossini, D., Vallenari, A., Bragaglia, A. et al. (2019). Age determination for 269 Gaia DR2 open clusters. *Astronomy and Astrophysics*, 623, A108. doi:10.1051/0004-6361/201834693.
- Bostanci, Z. F., Ak, T., Yontan, T. et al. (2015). A comprehensive study of the open cluster NGC 6866. *Monthly Notices of the Royal Astronomical Society*, 453(1), 1095–1107. doi:10.1093/mnras/stv1665.
- Bovy, J. (2015). galpy: A python library for Galactic dynamics. *The Astrophysical Journal Supplement Series*, 216(2), 29. doi:10.1088/0067-0049/216/2/29.
- Bovy, J., & Tremaine, S. (2012). On the local dark matter density. *The Astrophysical Journal*, 756(1), 89. doi:10.1088/0004-637X/756/1/89.
- Bressan, A., Marigo, P., Girardi, L. et al. (2012). PARSEC: stellar tracks and isochrones with the Padova and TRieste Stellar Evolution Code. *Monthly Notices of the Royal Astronomical Society*, 427(1), 127–145. doi:10.1111/j.1365-2966.2012.21948.x.
- Bukowiecki, L., Maciejewski, G., Konorski, P. et al. (2011). Open Clusters in 2MASS Photometry. I. Structural and Basic Astrophysical Parameters. *Acta Astronomica*, 61(3), 231–246. doi:10.48550/arXiv.1107.5119.
- Cantat-Gaudin, T., & Anders, F. (2020). Clusters and mirages: cataloguing stellar aggregates in the Milky Way. *Astronomy and Astrophysics*, 633, A99. doi:10.1051/0004-6361/201936691.
- Cantat-Gaudin, T., Anders, F., Castro-Ginard, A. et al. (2020). Painting a portrait of the galactic disc with its stellar clusters. *Astronomy and Astrophysics*, 640, A1. doi:10.1051/0004-6361/202038192.
- Cantat-Gaudin, T., Jordi, C., Vallenari, A. et al. (2018). A Gaia DR2 view of the open cluster population in the Milky Way. *Astronomy and Astrophysics*, 618, A93. doi:10.1051/0004-6361/201833476.
- Carraro, G., Sales Silva, J. V., Moni Bidin, C. et al. (2017). Galactic Structure in the Outer Disk: The Field in the Line of Sight to the Intermediate-age Open Cluster Tomabaugh 1. *The Astronomical Journal*, 153(3), 99. doi:10.3847/1538-3881/153/3/99.
- Casamiuela, L., Carrera, R., Blanco-Cuaresma, S. et al. (2017). OCCASO - II. physical parameters and Fe abundances of red clump stars in 18 open clusters. *Monthly Notices of the Royal Astronomical Society*, 470(4), 4363–4381. doi:10.1093/mnras/stx1481.
- Casamiuela, L., Carrera, R., Jordi, C. et al. (2016). The OCCASO survey: presentation and radial velocities of 12 Milky Way open clusters. *Monthly Notices of the Royal Astronomical Society*, 458(3), 3150–3167. doi:10.1093/mnras/stw518.
- Castro-Ginard, A., Jordi, C., Luri, X. et al. (2020). Hunting for open clusters in Gaia DR2: 582 new open clusters in the Galactic disc. *Astronomy and Astrophysics*, 635, A45. doi:10.1051/0004-6361/201937386.
- Castro-Ginard, A., Jordi, C., Luri, X. et al. (2019). Hunting for open clusters in Gaia DR2: the Galactic anticentre. *Astronomy and Astrophysics*, 627, A35. doi:10.1051/0004-6361/201935531.
- Castro-Ginard, A., Jordi, C., Luri, X. et al. (2018). A new method for unveiling open clusters in Gaia. new nearby open clusters confirmed by DR2. *Astronomy and Astrophysics*, 618, A59. doi:10.1051/0004-6361/201833390.
- Chen, B., Stoughton, C., Smith, J. A. et al. (2001). Stellar Population Studies with the SDSS. I. The Vertical Distribution of Stars in the Milky Way. *The Astrophysical Journal*, 553(1), 184–197. doi:10.1086/320647.
- Chincarini, G. (1966). The galactic cluster NGC 7762. *Memorie della Societa Astronomica Italiana*, 37, 423–425.
- Coşkunoğlu, B., Ak, S., Bilir, S. et al. (2011). Local stellar kinematics from RAVE data - I. Local standard of rest. *Monthly Notices of the Royal Astronomical Society*, 412(2), 1237–1245. doi:10.1111/j.1365-2966.2010.17983.x.
- Cuffey, J., & Shapley, H. (1937). Red indices in galactic clusters. *Annals of Harvard College Observatory*, 105(21), 403–444.
- de la Fuente Marcos, R., & de la Fuente Marcos, C. (2009). Double or binary: on the multiplicity of open star clusters*. *A&A*, 500(2), L13–L16. URL: <https://doi.org/10.1051/0004-6361/200912297>. doi:10.1051/0004-6361/200912297.
- Dias, W. S., Monteiro, H., Moitinho, A. et al. (2021). Updated parameters of 1743 open clusters based on Gaia DR2. *Monthly Notices of the Royal Astronomical Society*, 504(1), 356–371. doi:10.1093/mnras/stab770.
- Dias, W. S., Monteiro, H., Caetano, T. C. et al. (2014). Proper motions of the optically visible open clusters based on the UCAC4 catalog. *Astronomy and Astrophysics*, 564(1), A79. doi:10.1051/0004-6361/201323226.
- Donor, J., Frinchaboy, P. M., Cunha, K. et al. (2020). The open cluster chemical abundances and mapping survey. IV. abundances for 128 open clusters using SDSS/APOGEE DR16. *The Astronomical Journal*, 159(5), 199. URL: <https://dx.doi.org/10.3847/1538-3881/ab77bc>. doi:10.3847/1538-3881/ab77bc.
- Dreyer, J. L. E. (1888). A New General Catalogue of Nebulae and Clusters of Stars, being the Catalogue of the late Sir John F. W. Herschel, Bart, revised, corrected, and enlarged. *Memoirs of the Royal Astronomical Society*, 49, 1.
- Eker, Z., Bakış, V., Bilir, S. et al. (2018). Interrelated main-sequence mass-luminosity, mass-radius, and mass-effective temperature relations. *Monthly Notices of the Royal Astronomical Society*, 479(4), 5491–5511. doi:10.1093/mnras/sty1834.
- Eker, Z., Soydoğan, F., Bilir, S. et al. (2020). Empirical bolometric correction coefficients for nearby main-sequence stars in the Gaia era. *Monthly Notices of the Royal Astronomical Society*, 496(3), 3887–3905. doi:10.1093/mnras/staa1659.
- Gaia Collaboration, Brown, A. G. A., Vallenari, A. et al. (2018). Gaia Data Release 2. Summary of the contents and survey properties. *Astronomy and Astrophysics*, 616, A1. doi:10.1051/0004-6361/201833051.
- Gaia Collaboration, Brown, A. G. A., Vallenari, A. et al. (2021). Gaia Early Data Release 3. summary of the contents and survey properties. *Astronomy and Astrophysics*, 649, A1. doi:10.1051/0004-6361/202039657.
- Gaia Collaboration, Prusti, T., de Bruijne, J. H. J. et al. (2016). The Gaia mission. *Astronomy and Astrophysics*, 595, A1. doi:10.1051/0004-6361/201629272.
- Gaia Collaboration, Vallenari, A., Brown, A. G. A. et al. (2022). Gaia Data Release 3: Summary of the content and survey properties. *arXiv e-prints*, (p. arXiv:2208.00211). doi:10.48550/arXiv.2208.00211.
- Galadi-Enriquez, D., Jordi, C., & Trullols, E. (1998a). The overlapping open clusters NGC 1750 and NGC 1758. III. Cluster-field segregation and clusters physical parameters. *Astronomy and Astrophysics*, 337, 125–140.
- Galadi-Enriquez, D., Jordi, C., & Trullols, E. (1999). Astrometry and photometry of open clusters: NGC 1746, NGC 1750 and NGC 1758. *Astrophysics and Space Science*, 263(1), 307–310.
- Galadi-Enriquez, D., Jordi, C., Trullols, E. et al. (1998b). The overlapping open clusters NGC 1750 and NGC 1758. I. UBVR-I-CCD photometry. *Astronomy and Astrophysics*, 333, 471–478.
- Hopkins, A. M. (2018). The Dawes review 8: Measuring the stellar initial mass function. *Publications of the Astronomical Society of Australia*, 35, e039. doi:10.1017/pasa.2018.29.
- Hoskin, M. (2006). Caroline Herschel's catalogue of nebulae. *Journal for the History of Astronomy*, 37, 251–255. doi:10.1177/002182860603700301.
- Joshi, Y. C., Dambis, A. K., Pandey, A. K. et al. (2016). Study of open clusters within 1.8 kpc and understanding the Galactic structure. *Astronomy and Astrophysics*, 593(1), A116. doi:10.1051/0004-6361/201628944.
- Karaali, S., Ak, S. G., Bilir, S. et al. (2003a). A charge-coupled device study of high-latitude Galactic structure: testing the model parameters. *Monthly Notices of the Royal Astronomical Society*, 343(3), 1013–1024. doi:10.1046/j.1365-8711.2003.06743.x.

- Karaali, S., Bilir, S., Ak, S. et al. (2011). An improved metallicity calibration with UVB photometry. *Publications of the Astronomical Society of Australia*, 28(2), 95–106. doi:10.1071/AS10026.
- Karaali, S., Bilir, S., Karatas, Y. et al. (2003b). New metallicity calibration down to [Fe/H] = -2.75 dex. *Publications of the Astronomical Society of Australia*, 20(2), 165–172. doi:10.1071/AS02028.
- Kharchenko, N. V., Piskunov, A. E., Röser, S. et al. (2005). Astrophysical parameters of Galactic open clusters. *Astronomy and Astrophysics*, 438(3), 1163–1173. doi:10.1051/0004-6361/20042523.
- Kharchenko, N. V., Piskunov, A. E., Schilbach, E. et al. (2013). Global survey of star clusters in the Milky Way. II. the catalogue of basic parameters. *Astronomy and Astrophysics*, 558(1), A53. doi:10.1051/0004-6361/201322302.
- King, I. (1962). The structure of star clusters. I. an empirical density law. *Astronomical Journal*, 67, 471. doi:10.1086/108756.
- King, I. R., Bedin, L. R., Piotto, G. et al. (2005). Color-Magnitude Diagrams and Luminosity Functions Down to the Hydrogen-Burning Limit. III. A Preliminary Hubble Space Telescope Study of NGC 6791. *The Astronomical Journal*, 130(2), 626–634. doi:10.1086/431327.
- Koç, S., Yontan, T., Bilir, S. et al. (2022). A Photometric and Astrometric Study of the Open Clusters NGC 1664 and NGC 6939. *The Astronomical Journal*, 163(4), 191. doi:10.3847/1538-3881/ac58a0.
- Krone-Martins, A., & Moitinho, A. (2014). UPMASK: unsupervised photometric membership assignment in stellar clusters. *Astronomy and Astrophysics*, 561, A57. doi:10.1051/0004-6361/201321143.
- Krumholz, M. R., McKee, C. F., & Bland-Hawthorn, J. (2019). Star clusters across cosmic time. *Annual Review of Astronomy and Astrophysics*, 57(1), 227–303. doi:10.1146/annurev-astro-091918-104430.
- Landolt, A. U. (2009). UBVRI photometric standard stars around the celestial equator: Updates and additions. *The Astronomical Journal*, 137(5), 4186–4269. doi:10.1088/0004-6256/137/5/4186.
- Landolt, A. U., & Africano, J. L. (2010). Photometry of a group of stars in the direction of NGC 1746/1750/1758. *Publications of the Astronomical Society of the Pacific*, 122(895), 1008. URL: <https://dx.doi.org/10.1086/656322>. doi:10.1086/656322.
- Lindoff, U. (1968). The ages of open clusters. *Arkiv for Astronomi*, 5(1), 1–21.
- Liu, L., & Pang, X. (2019). A Catalog of Newly Identified Star Clusters in Gaia DR2. *The Astrophysical Journal Supplement Series*, 245(2), 32. doi:10.3847/1538-4365/ab530a.
- Loktin, A. V., & Popova, M. E. (2017). Updated version of the 'homogeneous catalog of open cluster parameters'. *Astrophysical Bulletin*, 72(3), 257–265. doi:10.1134/S1990341317030154.
- Maciejewski, G., Boeva, S., Georgiev, T. et al. (2008). Photometric study of open clusters NGC 2266 and NGC 7762. *Baltic Astronomy*, 17, 51–65.
- Maciejewski, G., & Niedzielski, A. (2007). CCD BV survey of 42 open clusters. *Astronomy and Astrophysics*, 467(3), 1065–1074. doi:10.1051/0004-6361:20066588.
- Majewski, S. R. (1993). Galactic structure surveys and the evolution of the Milky Way. *Annual Review of Astronomy and Astrophysics*, 31, 575–638. doi:10.1146/annurev.aa.31.090193.003043.
- Miyamoto, M., & Nagai, R. (1975). Three-dimensional models for the distribution of mass in galaxies. *Publications of the Astronomical Society of Japan*, 27, 533–543.
- Navarro, J. F., Frenk, C. S., & White, S. D. M. (1996). The Structure of Cold Dark Matter Halos. *Astrophysical Journal*, 462, 563. doi:10.1086/177173.
- Patát, F., & Carraro, G. (1995). NGC 7762: A forgotten moderate age open cluster. *Astronomy and Astrophysics Supplement*, 114, 281.
- Poggio, E., Drimmel, R., Cantat-Gaudin, T. et al. (2021). Galactic spiral structure revealed by Gaia EDR3. *Astronomy and Astrophysics*, 651, A104. URL: <https://doi.org/10.1051/0004-6361/202140687>. doi:10.1051/0004-6361/202140687.
- Reddy, A. B. S., & Lambert, D. L. (2019). Comprehensive abundance analysis of red giants in the open clusters Stock 2, NGC 2168, 6475, 6991, and 7762. *Monthly Notices of the Royal Astronomical Society*, 485(3), 3623–3641. doi:10.1093/mnras/stz468.
- Sampedro, L., Dias, W. S., Alfaro, E. J. et al. (2017). A multimembership catalogue for 1876 open clusters using UCAC4 data. *Monthly Notices of the Royal Astronomical Society*, 470(4), 3937–3945. doi:10.1093/mnras/stx1485.
- Scalo, J. (1998). The IMF Revisited: A Case for Variations. In G. Gilmore, & D. Howell (Eds.), *The Stellar Initial Mass Function (38th Hermonceux Conference)* (p. 201). volume 142 of *Astronomical Society of the Pacific Conference Series*. doi:10.48550/arXiv.astro-ph/9712317.
- Soubiran, C., Cantat-Gaudin, T., Romero-Gómez, M. et al. (2018). Open cluster kinematics with Gaia DR2. *Astronomy and Astrophysics*, 619, A155. doi:10.1051/0004-6361/201834020.
- Stetson, P., Pancino, E., et al. (2019). Homogeneous photometry - vii. globular clusters in the gaia era. *Monthly Notices of the Royal Astronomical Society*, 485, 3042–3063. doi:10.1093/mnras/stz585.
- Straizys, V. (1992). *Multicolor stellar photometry*. Tucson: Pachart Pub. House.
- Straizys, V., Kazlauskas, A., Černiauskas, A. et al. (2003). Overlapping Open Clusters NGC 1750 and NGC 1758 Behind the Taurus Dark Clouds. II. CCD Photometry in the Vilnius System. *Baltic Astronomy*, 12, 323–351. doi:10.1515/astro-2017-0055.
- Straizys, V., Cernis, K., & Maistas, E. (1992). Probable open clusters NGC 1750 and NGC 1758 behind the Taurus Dark Clouds. *Baltic Astronomy*, 1, 125–141. doi:10.1515/astro-1992-0201.
- Sun, M., Jiang, B., Yuan, H. et al. (2021). The ultraviolet extinction map and dust properties at high galactic latitude. *The Astrophysical Journal Supplement Series*, 254(2), 38. doi:10.3847/1538-4365/abf929.
- Sung, H., Lim, B., Bessell, M. S. et al. (2013). Sejong open cluster survey (SOS). 0. target selection and data analysis. *Journal of Korean Astronomical Society*, 46(3), 103–123. doi:10.5303/JKAS.2013.46.3.103.
- Szabo, R. (1999). New variable stars in NGC 7762. *Information Bulletin on Variable Stars*, 4700, 1.
- Tarricq, Y., C., S., Casamiquela, L. et al. (2021). 3D kinematics and age distribution of the open cluster population. *Astronomy and Astrophysics*, 647, A19. doi:10.1051/0004-6361/202039388.
- Tian, K.-P., Zhao, J.-L., Shao, Z.-Y. et al. (1998). Determination of proper motions and membership of the open clusters ngc 1750 and ngc 1758. *Astronomy and Astrophysics Supplement*, 131(1), 89–98. URL: <https://doi.org/10.1051/aas:1998253>. doi:10.1051/aas:1998253.
- Wang, H., Zhang, Y., Zeng, X. et al. (2022). Searching for variable stars in the open cluster NGC 2355 and its surrounding region. *The Astronomical Journal*, 164(2), 40. doi:10.3847/1538-3881/ac755a.
- Yontan, T. (2023). An investigation of open clusters Berkeley 68 and Stock 20 using CCD UVB and Gaia DR3 data. *The Astronomical Journal*, (p. arXiv:2211.09825). doi:10.48550/arXiv.2211.09825.
- Yontan, T., Bilir, S., Ak, T. et al. (2021). A study of open clusters Frolow 1 and NGC 7510 using CCD UVB photometry and Gaia DR2 astrometry. *Astronomische Nachrichten*, 342(3), 538–552. doi:10.1002/asna.202113837.
- Yontan, T., Bilir, S., Bostanci, Z. F. et al. (2019). CCD UVB photometric and Gaia astrometric study of eight open clusters — ASCC 115, Collinder 421, NGC 6793, NGC 7031, NGC 7039, NGC 7086, Roslund 1 and Stock 21. *Astrophysics and Space Science*, 364(9), 152. doi:10.1007/s10509-019-3640-y.
- Yontan, T., Bilir, S., Bostanci, Z. F. et al. (2015). CCD UVBRI photometry of NGC 6811. *Astrophysics and Space Science*, 355(2), 267–281. doi:10.1007/s10509-014-2175-5.